Development of therapeutic strategy for infectious diseases using the antimicrobial peptide or receptor antagonist

（抗菌ペプチドと受容体拮抗剤を用いた

感染症治療法の開発）

Akira Kawaguchi

Department of Molecular Pathobiology,
Research Center for Zoonosis Control,
HokkaidoUniversuity

Contents

List of Abbreviations

AMPs	**Antimicrobial peptides**
APD	**Antimicrobial peptide database**
ATL	**Adult T-cell leukemia**
bp	**basepair**
CD	**Circular dichroism**
cDNA	**complementary DNA**
CFU	**Colony forming units**
CTACK	**cutaneous T cell-attracting chemokine**
DMEM	**Dulbecco's modified Eagle's medium**
DMSO	**dimethyl sulfoxide**
FBS	**Fetal bovine serum**
GPCR	**G protein-coupled receptors**
h	**hour**
H&E	**Hematoxylin and eosin**
HTLV-I	**Human T lymphotropic virus-type I**
LARC	**Liver and Activation Regulated Chemokine**
MEM	**Minimum essential medium**
min	**minute**
MIP-3α	**Macrophage inflammatory protein-3α**
PBS	**Phosphate-buffered saline**

PCR	**Polymerase chain reaction**
PI3K	**Phosphatidylinositol 3 kinase**
pML cell	**Primary murine lymphoblastoid cell**
RANTES	**Regulated on activation normal T expressed and secreted**
RPMI	**Roswell park memorial institute**
RT	**Reverse transcription**
S. aureus	***Staphylococcus aureus***
SCID	**Severe combined immunodeficiency**
SDF-1α	**Stromal-cell derived factor-1α**
SDS	**Sodium dodecyl sulfate**
sec	**second**
SLC	**Secondary Lymphoid-tissue Chemokine**
S. typhimurium	***Salmonella enterica* serovar Typhimurium**
TARC	**Thymus and Activation Regulated Chemokine**
TFE	**Trifluoroethanol**
TSA	**Tryptic soy agar**
TSB	**Tryptic soy broth**

Preface

Infectious diseases are still one of the most important causes of morbidity and mortality of people and animals all over the world. Epidemiological research and development of vaccine are important as primary prevention for the infectious diseases. Because the primary prevention is not sufficient to overcome the infectious diseases, secondary prevention, including development of prophylactic and therapeutic strategy is also important. However, the therapeutic strategy is not well established for many infectious diseases, therefore it is necessary to establish effective therapeutic approach for the infectious diseases.

In the chapter I, I examined the efficacy of antimicrobial peptides (AMPs) against bacterial infection. AMPs play pivotal role in innate immunity that is non-specific and fast-acting defense system against infection and bind to bacterial membrane, resulting in bactericidal activity. For this non-specific defense activity, it is suggested that the emergence of AMPs–resistant bacteria rarely occur and AMPs may be useful for therapeutic strategy for infectious diseases.

I isolated a novel gene that is similar to mouse β–defensins which are one of the family of AMPs, and observed that the location of this gene in mouse genome and the characteristics of its gene structure are very common to that of β-defensins. Moreover, I predicted the region corresponding to the mature peptide of this gene, synthesized a small peptide based on this sequence, designated as K17, and analyzed structure and

function of the small peptide. This peptide has positive charge as same as known AMPs. Circular dichroism (CD) spectroscopy analysis of K17 demonstrated that K17 presents random coil conformation in aqueous solution, but adopts α-helical conformation in a membrane-mimicking environment. K17 exhibited bactericidal activity against *Salmonella enterica* serovar Typhimurium (Gram negative) and *Staphylococcus aureus* (Gram positive), but it was not cytotoxic in cultures of mammalian cells or hemolytic in cultures of erythrocytes. From these results, it is suggested that the peptide (K17) which I synthesized in this study may be a candidate therapeutic for the treatment of infectious diseases.

In the chapter II, I aimed at the host response occurred after the development of Adult T-cell Leukemia (ATL). ATL is the T-cell malignancy caused by Human T-cell leukemia virus type-I (HTLV-I) that belongs to retrovirus. Because there is no effective ATL therapy, the development of therapy is needed. A characteristic manifestation of ATL is extensive infiltration of leukemic cells into various organs, including lymph nodes, liver, spleen, lungs, and skin. The molecular mechanisms associated with ATL cell infiltration are poorly understood. Therefore, the investigation of the infiltration mechanism may be important for development of ATL therapy. Because tumor cells are attracted to several tissues by chemokine expressing in those tissues, I examined the response of ATL cells to several chemokines and found that ATL cells show markedly response to stromal-cell derived factor-1α (SDF-1α). AMD3100, the antagonist against CXCR4 that is receptor for SDF-1α, suppressed the responsibility and the infiltration of

ATL cells to tissues in mouse model. These results suggest the SDF-1α/CXCR4 interaction involves in leukemic cell migration and this pathway may become a novel candidate target for ATL therapy.

In the chapter I and II, I demonstrated development of therapeutic approaches for infectious diseases.

[Chapter 1]

Bactericidal activity of the peptide derived from a novel mouse defensin-like gene

(Functional analysis of an α-helical antimicrobial peptide derived from a novel mouse defensin-like gene)

Introduction

Innate immunity in animals depends in large part on the activity of non-specific effector molecules. In particular, gene-encoded antimicrobial peptides (AMPs) are now clearly established as key players in both plant and animal defense systems. Despite broad divergence in sequence and taxonomy, most AMPs share a common mechanism of action involving membrane permeabilization of the pathogen cell membrane. Importantly, AMPs are recognized as a potential source of therapeutic drugs for the treatment of antibiotic-resistant bacterial infections.

To date, more than 880 different AMPs have been identified or predicted based on nucleic acid sequences. These include AMPs that are produced in many tissues and cell

types in a variety of invertebrate, plant and animal species, as well as certain cytokines and chemokines. AMPs are a unique and diverse group of molecules that can be divided into subgroups based on amino acid composition and structure [1, 2]. The subgroup of anionic AMPs includes small peptides present in surfactant extracts, bronchoalveolar lavage fluid, and airway epithelial cells. A second subgroup is comprised of approximately 290 linear cationic α-helical peptides. These peptides are short, lack cysteine residues and may possess a hinge or kink in the middle of the peptide. In aqueous solution, many of these peptides are disordered, but in the presence of trifluoroethanol (TFE) or sodium dodecyl sulfate (SDS) micelles, all or part of the molecules are converted to an α-helical conformation [1, 2]. For some of the members of this subgroup, α-helicity correlates with antimicrobial activity. A third subgroup contains approximately 44 cationic peptides that are rich in certain amino acids. This group includes the bactenecins and PR-39, which are rich in proline and arginine residues. Peptides in this group lack cysteine residues and are linear, although some can form extended coils. A forth subgroup of approximately 380 members consists of anionic and cationic peptides that contain cysteine residues and form disulfide bonds and stable β-sheets. This subgroup includes the diverse family of defensins and protegrin. There are approximately 55 α-defensins, 90 β-defensins, 54 arthropod (insect) defensins, and 58 plant defensins; a rhesus θ-defensin has also been identified.

Using a set of primers designed to amplify conserved mouse β-defensin sequences located outside of the translated region, we identified a novel small gene with an open reading frame of 114 basepairs (bp) and a predicted amino acid sequence of 37 residues.

A search of the genome database (http://www.ensembl.org) revealed that the gene locus and exon 1 sequence of this novel gene were similar to subgroup 1 mouse β-defensins. We designated this gene mouse β-defensin-like small (m*BDLs*).

The β-defensin genes consist of two exons. Exon 1 encodes a signal sequence and exon 2 encodes the pro and mature peptides that function as AMPs. The gene structure of m*BDLs* was similar to other β-defensins, which suggested that the mature peptide was encoded by exon 2. We synthesized a small peptide, K17, based on the nucleotide sequence of exon 2. K17 lacked cysteine residues. The peptide showed random coil conformation in aqueous solution, but formed α-helical structure in the presence of 50% TFE and 1% SDS, a membrane-mimicking environment, as identified by circular dichroism (CD) spectroscopy. The antimicrobial activity of K17 was assessed to determine if it functioned as an α-helical AMP. K17 exhibited bactericidal activity against Gram negative *Salmonella enterica* serovar Typhimurium and Gram positive *Staphylococcus aureus* at a concentration that is typical for other defensins. K17 did not exhibit cytotoxicity against normal or transformed mammalian cells (NIH3T3, HeLa, and A549 cells) or hemolytic activity against mouse erythrocytes at concentrations that inhibited bacterial growth. These results suggested that K17 may be a candidate therapeutic for the treatment of bacterial infections.

Materials and methods

Tissue samples

Murine tissues were obtained from adult C57BL/6 mice. All animal experiments were approved by the Animal Care and Use Committee of the National Institute of Infectious Diseases.

Reverse transcriptase (RT)-PCR

Total RNA was isolated from mouse brain tissue using Trizol (Invitrogen, Carlsbad, CA). Complementary DNA (cDNA) was generated by Omniscript RT-PCR (Qiagen, Valencia, CA) and used as a template for RT-PCR. The PCR conditions were as follows: 95 °C for 2 min, followed by 30 cycles of 95°C for 30 sec, 55°C for 30 sec and 72°C for 1 min, then 72°C for 7 min. The primers (5′-CAGTCATGAGGATCCATTAC-3′ and 5′-CATGGAGGAGCAAATTCTGG-3′) were designed to target a conserved region of the mouse β-defensin gene sequence. PCR products were separated by agarose gel electrophoresis, stained with ethidium bromide and then visualized under UV illumination.

5′-Rapid amplification of cDNA ends (RACE) and sequencing

To isolate the full-length cDNA for m*BDLs*, we performed 5′-RACE using the 5′-Full RACE core kit (Takara, Tokyo, Japan) and the following primers: S1, 5′-TAGCCCTCAAATGCTGCAAG-3′; A1, 5′-AAGCTGCAAATGGAGACAGC-3′; S2,

5′-AGACAAAGATCCTGTGAACC-3′; and A2, 5′-GCAACACCAGGAGAAATGAG-3′. PCR products were separated on a 2.0% agarose gel and the band of the expected size was removed, purified with a Qiaquick Gel Extraction Kit (Qiagen) and then subcloned into pGEM-T easy (Promega, Madison, WI). The cloned DNA sequence was confirmed by cycle sequencing using the Big Dye Terminator v1.1/3.1Cycle Sequencing Kit (Applied Biosystems, Foster City, CA) and a 3100-Avant Genetic Analyzer (Applied Biosystems).

Genome, sequence, phylogenetic, and secondary structure analyzes

Genome analysis of the cloned cDNA and its locus was carried out using BLAST searches of the Ensembl genome database (http://www.ensembl.org). DNASIS pro software (Hitachi Software Engineering, Tokyo, Japan) was used to predict amino acid sequences and perform sequence comparisons. Genetyx software (Genetyx Corporation, Tokyo, Japan) was used to construct the phylogenetic tree of m*BDLs* and five members of subgroup 1 mouse β-defensins. The PEP-FOLD Server (http://bioserv.rpbs.univ-paris-diderot.fr/PEP-FOLD) and Antimicrobial Peptide Database (APD; http://aps.unmc.edu/AP/main.html) were used to predict three-dimensional (3D) conformations and predict antimicrobial function, respectively.

Peptide synthesis

Based on the predicted amino acid sequence of m*BDLs*, the small peptide K17 (FSPQMLQDIIEKKTKIL) and the K17 analog A17, which contained three

lysine-to-alanine substitutions (FSPQMLQDIIEAATAIL) were chemically synthesized by Sigma Genosys (Ishikari, Japan).

Bactericidal assay

Bactericidal assays were performed using wild-type and defensin-sensitive *phoP* strains of *S. enterica* serovar Typhimurium (*S.* Typhimurium) and *Staphylococcus aureus* (*S. aureus*), as described previously [4]. Bacteria were stored at −80°C in cryopresevant. All assays were performed in duplicate. Bacteria were cultured in tryptic soy broth (TSB). One thousand colony forming units (CFU), as determined by the OD of exponentially growing cultures, were collected by centrifugation and then resuspended in 25 μl of distilled water. Various concentrations of peptide were added to the cells, and the suspension was allowed to incubate for 60 min at 37°C, at which point CFU were quantified by growth on tryptic soy agar (TSA) plates at 37°C overnight. The number of CFU of treated samples was compared to controls without peptide.

Growth inhibitory activity against tumor and normal fibroblast cells

Cells were grown in DMEM supplemented with 10% heat-inactivated fetal bovine serum (FBS), 100 units/ml penicillin G, and 100 μg/ml streptomycin. Cells were plated on 96-well plates at a concentration of 6×10^3 cells/100 μl in the same medium. After incubating the plates overnight at 37°C in an atmosphere of 5% CO_2, the medium was changed to OPTI-Pro without FBS. Ten microliters of diluted peptide were added to the cells, and then the plates were incubated for 24 h, at which point 50 μl of XTT solution

from the Cell proliferation kit II [XTT] (Roche Diagnostics, Indianapolis, IN) were added to each well. The plates were incubated for an additional 3 h, and then absorbance was measured at 490 nm using a microplate ELISA reader (Bio-Rad Laboratories, Hercules, CA).

Hemolysis assay

Hemolytic activity was evaluated by measuring hemoglobin release from fresh mouse erythrocytes. Mouse red blood cells were isolated using a cellulose column. Erythrocytes were suspended in phosphate buffered saline (PBS; 100 μl) (8% v/v) and then plated on 96-well U-bottomed plates (Nunc, Roskilde, Denmark). Ten microliters of peptide dissolved in PBS were added to each well, and then the plates were incubated for 1 h at 37°C, after which they were subjected to centrifugation at 1500 *g* for 5 min. The supernatant (100 μl) was then transferred to a 96-well microtiter plate. Hemolysis was monitored by absorbance at 414 nm with an ELISA plate reader (Bio-Rad). Complete hemolysis (set as 100%) was achieved by the addition of Triton X-100 at a final concentration of 0.01%. Hemolysis percentage was calculated according to the following equation: % hemolysis = [(Ab_{414} nm in peptide solution − Ab_{414} nm in PBS)/(Ab_{414} nm in 0.1% Triton X-100 − Ab_{414} nm in PBS)] × 100.

CD spectroscopy

The far-UV CD spectra of K17 and A17 were recorded in a J-805 spectropolarimeter (Jasco, Tokyo, Japan) at room temperature using 0.2 cm path length

quartz cuvette. Both peptides were dissolved in either distilled water, 1% SDS, or 50% TFE at final concentrations of 50 and 100 μg/ml for K17 and A17, respectively.

Statistics

Experimental groups were compared statistically using the Student's *t*-test. A *p* value of <0.05 was considered statistically significant.

Results

Identification of the m*BDLs* gene

RT-PCR analysis of a mouse brain cDNA library was carried out using primers that were specific for conserved mouse β-defensin sequences located outside of the translated region. Amplified products were separated by agarose gel electrophoresis and a small band of approximately 150 bp, which was similar to the expected size of mouse β-defensin genes, was detected (data not shown). To characterize this small PCR product, the amplified fragment was subcloned and sequenced. Analysis by 5′-RACE using a primer designed to target the coding region revealed that the small cDNA contained a 114 bp open reading frame encoding a putative peptide of 37 amino acid residues (Figure 1A).

In silico genome scan

The small cDNA sequence was verified using the Emsembl BLASTview program [5]. There was a 100% match between the isolated small cDNA and a locus on mouse chromosome 8 (database location: AC121131.14, 100856–100918). The gene contained two exons separated by one intron and was 1698 bp in length (Figure 1B). In exon 1, the 5′-untranslated region contained an NF-κB binding site and TATA box (Figure 1B). The gene structure was consistent with characteristics commonly found in mouse defensin genes, namely, two exons separated by an intron (1.7 kb) and an NF-κB binding site and TATA box in the 5′-untranslated region [6].

The A3 region on chromosome 8 is divided into two contigs that are separated by approximately 850 kb. The first contig contains six mouse β-defensin (mBD) genes, including mBD4, 6, 5, 3, and 7, as well as DefR1. These genes all belong to β-defensin subgroup 1. The small gene was located after mBD7 in the first contig (Figure 1C). Since the small gene had similar structural characteristics to other mouse β-defensins, it was designated m*BDLs*, for mouse β-defensin-like small gene.

Prediction of mBDLs amino acid sequence

The amino acid sequence of mBDLs was predicted and compared with other members of the mouse β-defensin family (Figure 2A). The cDNA sequence of m*BDLs* exhibited 60–80% similarity to other subgroup 1 members such as mBD3, mBD4, mBD5, mBD7, and DefR1, but lower homology to subgroup 2 members, including mBD2 and mBD10. The prepro region (amino acids 1–23) of the mBDLs peptide was

highly similar to subgroup 1 family members, but the level of similarity was lower for the mature peptide sequence (amino acids 24–66; Figure 2A). It has been reported that β-defensin subgroup 1 members contain similar signal sequences and are of similar exon length [7-9]. As both the sequence and length of m*BDLs* exon 1 were similar to other subgroup 1 members, we propose that it belongs to the same family. Phylogenetic analysis of mBDLs and five mouse subgroup 1 β-defensin genes showed that mBDLs forms a branch with mBD7, while mBD4 and mBD5 with mBD3 formed other branches (Figure 2B). Although mBDLs exhibited similarity to other β-defensin subgroup 1 family members with respect to gene locus and exon–intron structure, as well as by phylogenetic analysis, mBDLs was much smaller than these other defensins and did not contain cysteine residues.

Design of peptides and CD analysis of these peptides

The mature defensin peptide is encoded by exon 2 [8, 9]. Based on the predicted amino acid sequence of m*BDLs* exon 2, we synthesized a small peptide, termed K17 (FSPQMLQDIIEKKTKIL), and the K17 analog A17 (FSPQMLQDIIEAATAIL), which contained three alanines in place of the three lysine residues (Figure 3A). Structural analysis using PEP-FOLD, which builds on a new *de novo* approach to predicting 3D peptide structures from sequence information [3], indicated that K17 and A17 each adopt an α-helical conformation (Figures 3B and C). The secondary structures of these peptides were analyzed by a CD spectroscopy. The CD spectra of K17 and A17 dissolved in distilled water exhibited disordered as random coil (Figures 3D and E).

Upon the addition of 50% TFE or 1% SDS, a conformational change occurred, as evidenced by spectrum containing minima at 208 and 222 nm. Based on these spectra, these peptides adopted α-helical structure in the membrane-mimicking environment. The result is in good agreement with the results of other online prediction, Antimicrobial Peptide Database (APD) that predicts whether these peptides would have antimicrobial activity [10]. According to the APD, K17, which was cationic and could putatively interact with membranes, was predicted to function as an AMP, while A17, which had a net negative charge, would not.

Antimicrobial activity

The bactericidal activity of the two peptides was first examined using the defensin-sensitive *phoP* strain of *S.* Typhimurium. The lack of a *PhoP* system for antimicrobial resistance makes this strain a useful tool for determining the antimicrobial mechanisms of defensins [4]. At concentrations (5 and 10 μg/ml) that are generally considered optimal for the bactericidal activity of other AMPs, K17 exhibited dose-dependent bactericidal activity against the *phoP*-strain of *S.* Typhimurium, whereas there was no increase in activity in the presence of A17 (5 and 10 μg/ml) (Figure 4A). We next examined bactericidal activity against wild-type *S.* Typhimurium (Gram negative) and *S. aureus* (Gram positive). K17 showed significantly higher bactericidal activity against *S.* Typhimurium and *S. aureus* (approximately 40%) as compared to A17 (Figure 4B).

Cytotoxicity against mammalian tumor and normal cells

The cytotoxicity of K17 and A17 in mammalian cell cultures was investigated by growth inhibition of normal mouse NIH3T3 fibroblasts and two transformed tumor cell lines (HeLa and A549). Neither K17 nor A17 was cytotoxic in cultures of normal and tumor cells at concentrations of 2, 20, and 200 μg/ml (Figure 4C).

Hemolytic activity

The hemolytic activity of K17 and A17 was determined using mouse erythrocytes. No significant hemolytic activity of the peptides was observed at concentrations of 2, 20, and 200 μg/ml (Figure 4D).

Discussion

A mouse β-defensin-like gene was amplified from mouse brain using primers designed to target conserved mouse β-defensin gene sequences. This novel gene was designated mouse β-defensin-like small, or m*BDLs*. The genomic structure of m*BDLs* was similar to other subgroup 1 β-defensins in that it contained two exons separated by one intron, was approximately 2 kb [6, 11, 12] and contained an NF-κB binding site [6, 13, 14], and TATA box [11] in the 5′-untranslated region.

The β-defensin genes possess two exons and one intron. A signal sequence is encoded by exon 1 and the mature peptide is encoded by exon 2 [8]. Because the sequence of exon 1 of m*BDLs* was similar to other subgroup 1 members, we predicted that exon 2 would encode the mature peptide. We synthesized a small peptide, termed K17, derived from the nucleotide sequence of exon 2 of m*BDLs*. We also synthesized a K17 analog that contained alanine residues in place of lysine residues, termed A17. Replacement or deletion of specific amino acid residues in the original peptide is a common technique for analyzing new AMPs [15], such as cecroprins and maganines [16, 17]. K17 was cationic, lacked cysteine residues, and it was shown that the peptide exhibited α-helical conformation in lipid membrane-mimicking solvents such as 50% TFE or 1% SDS by CD spectroscopy. A17 was also adopted α-helical structure but had negative charge.

AMPs are divided into four subgroups based on amino acid composition and structure. One of AMPs subgroups is typically α-helical, short, cationic peptides that lack cysteine residues [1]. The characteristics of K17 were consistent with those of the AMP subgroup. Furthermore, the APD predicted that K17 would function as an AMP [10]. Examination of the antimicrobial activity of K17 and A17 against the *phoP*-strain of *S.* Typhimurium, which is sensitive to AMPs [4], and two wild-type strains (*S.* Typhimurium and *S. aureus*) showed that K17 had antimicrobial activity against Gram positive and Gram negative bacteria at concentrations that are generally considered optimal for the bactericidal activity of other AMPs. The K17 analog A17, which also adopted an α-helical conformation but lost charge due to replacement of lysines by

alanines, lacked antimicrobial activity. While the precise mechanism of action of AMPs is not fully understood [18], these results suggested that charge is related to antimicrobial activity, at least for K17. Although some α-helical antimicrobial peptides exert cytotoxic and hemolytic effects [19], K17 was not hemolytic in cultures of mouse erythrocytes or cytotoxic in cultures of NIH3T3, HeLa, or A549 cells. These results suggest that K17 is non-toxic to mammalian cells at concentrations that are bactericidal.

In summary, we have isolated a novel β-defensin-like gene, m*BDLs*, and have demonstrated that a peptide based on the m*BDLs* sequence possesses antimicrobial activity against both Gram negative and Gram positive bacteria. Although the peptide does not contain any cysteine residues, as do other defensins, it possesses many features that are characteristic of one of AMPs subgroups. As such, K17 represents a potential candidate therapeutic for the treatment of bacterial infections.

Summary

Gene-encoded antimicrobial peptides (AMPs) are an essential component of the innate immune system in many species. Analysis of β-defensin gene expression in mouse tissue using primers that were specific for conserved sequences located outside of the β-defensin translated region identified a novel small gene. The novel gene had an open reading frame of 114 basepairs and encoded a predicted protein of 37 amino acid

residues. A search of the genome database revealed that the gene locus and the sequence of exon 1 of this novel gene were similar to subgroup 1 mouse β-defensins. A small peptide, K17 (FSPQMLQDIIEKKTKIL), derived from the amino acid sequence of this novel gene was synthesized. Circular dichroism (CD) spectroscopic analysis of chemically synthesized peptide demonstrated that the peptide exhibited random coil conformation in aqueous solution, but the peptide adopted helical conformation in the presence of trifluoroethanol (TFE) or sodium dodecyl sulfate (SDS), a membrane mimicking environment. The peptide exhibited bactericidal activity against *Salmonella enterica* serovar Typhimurium (Gram negative) and *Staphylococcus aureus* (Gram positive); it was not cytotoxic in cultures of mammalian cells or hemolytic in cultures of erythrocytes. These results suggested that K17 might be a candidate therapeutic for the treatment of bacterial infection.

Figure 1

(A)

Sequence (114bp)

ATGAGGATCCGTTACCTTCTG
TTCTCATTTCTCCTGGTGTTG
CTGTCTCCATTTGCAGCTTTT
AGCCCTCAAATGCTGCAAGAT
ATAATAGAGAAGAAGACAAAG
ATCCTGTGA

Amino acid sequence
(37amino acids)

MRIRYLLFSFLLVLLSPFA
AFSPQMLQDIIEKKTKIL*

(B)

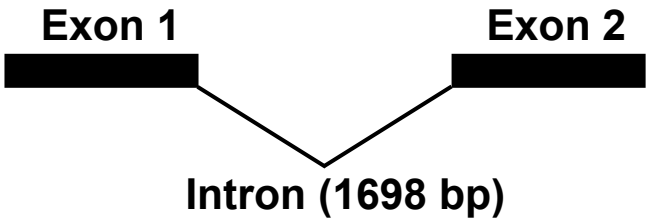

AACCAGTAAGTCTCTCCCAGGACAGCCTGGG
TCCCTCTCATGTAAGATGTAAGGCAGGAAGC
TGTTCTTGTTGAGCAGTGCAGGAGGAAATCA
CCTGGGGATCCTCACATTTGCATAAGAGACT
CTGAGTGTGCTCTCCAATGTCACCTTGACAA
GAGAGATAAGGTGCTCTGTGTTTCATAATTG
TAATTCCTTGGATTCAAGTCAGTGTAGAATC
CTACCGAGGAAGCAGCACCTGGCACTATATA
AGGCACTGAGCTCAAGTCCCTCTGCATCTCT
GTACCTCACCAGGCTTCAGTC

ATGAGGATCCGTTACCTTCTGTTCTCATTTC
TCCTGGTGTTGCTGTCTCCATTTGCAG

1698 bp of intron sequence

CTTTTAGCCCTCAAATGCTGCAAGATATAA
TAGAGAAGAAGACAAAGATCCTGTGA

NF-κB binding site
TATA box

(C)

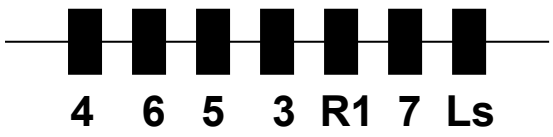

Figure 1 Structure of a small gene with homology to mouse β-defensins
(A) Nucleotide sequence of the small cDNA amplified using primers specific for conserved mouse β-defensin sequences, and the corresponding predicted amino acid sequence. * indicates the stop codon. (B) The full genomic sequence of the small gene. The gene contains 2 exons separated by 1 intron and is 1698 bp in length. A NF-κB binding site is underlined and a TATA box is double-underlined. Coding sequences are represented in bold and italic. (C) The small gene and other mouse β-defensins localize to the A3 region of chromosome 8 (Chr 8). The small gene is located after mBD7 in the first contig. 4, mBD4; 6, mBD6; 5, mBD5; 3, mBD3; R1, DefR1; 7, mBD7; Ls, mBDLs. .

Figure 2

(A)

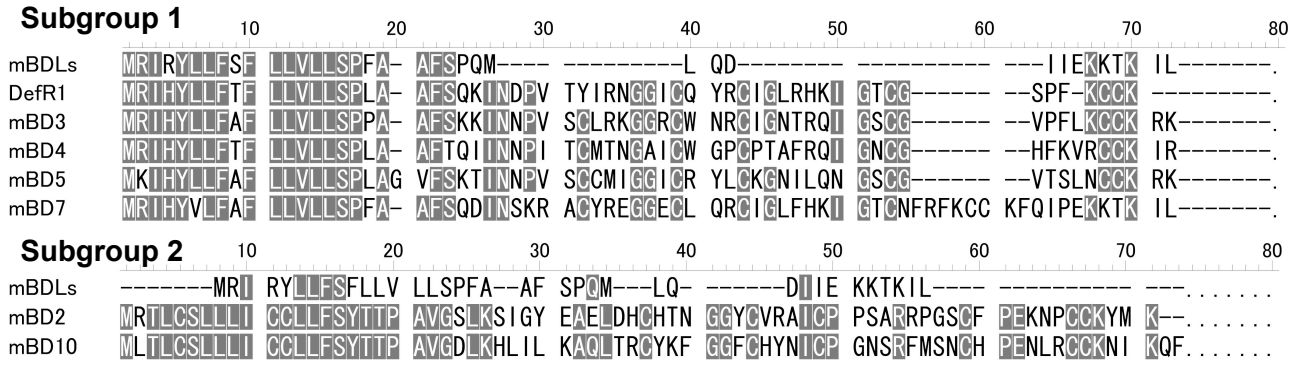

(B)

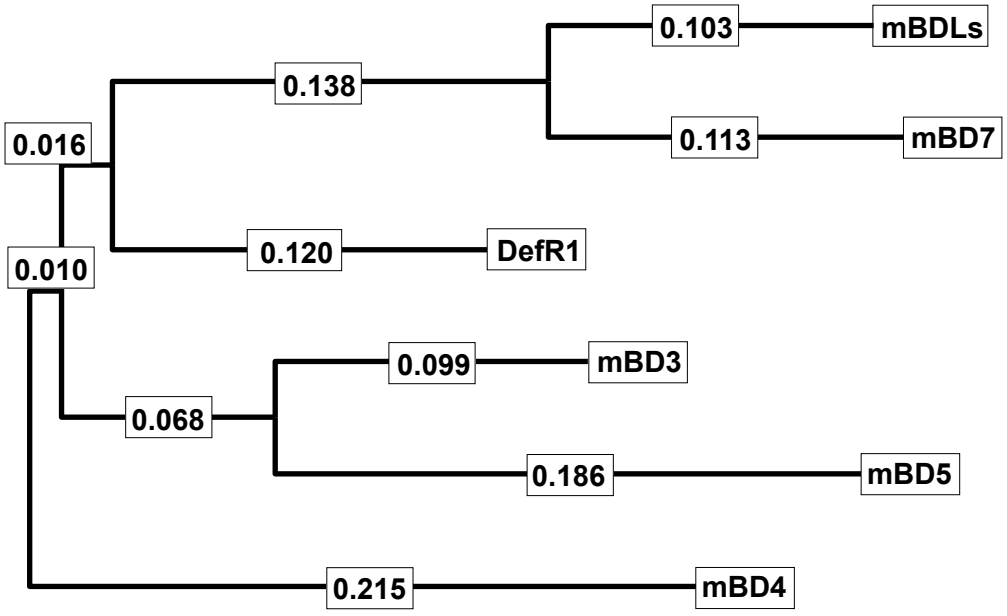

Figure 2 Comparison of the amino acid sequences of mBDLs and other mouse β-defensins
(A) Alignment of amino acid sequences of mBDLs and other mouse β-defensins of subgroups 1 and 2. Amino acid residues that are conserved in 80% of subgroup members are shaded in gray.
(B) Phylogenetic tree of mBDLs and 5 mouse β-defensins of subgroup 1.

Figure 3

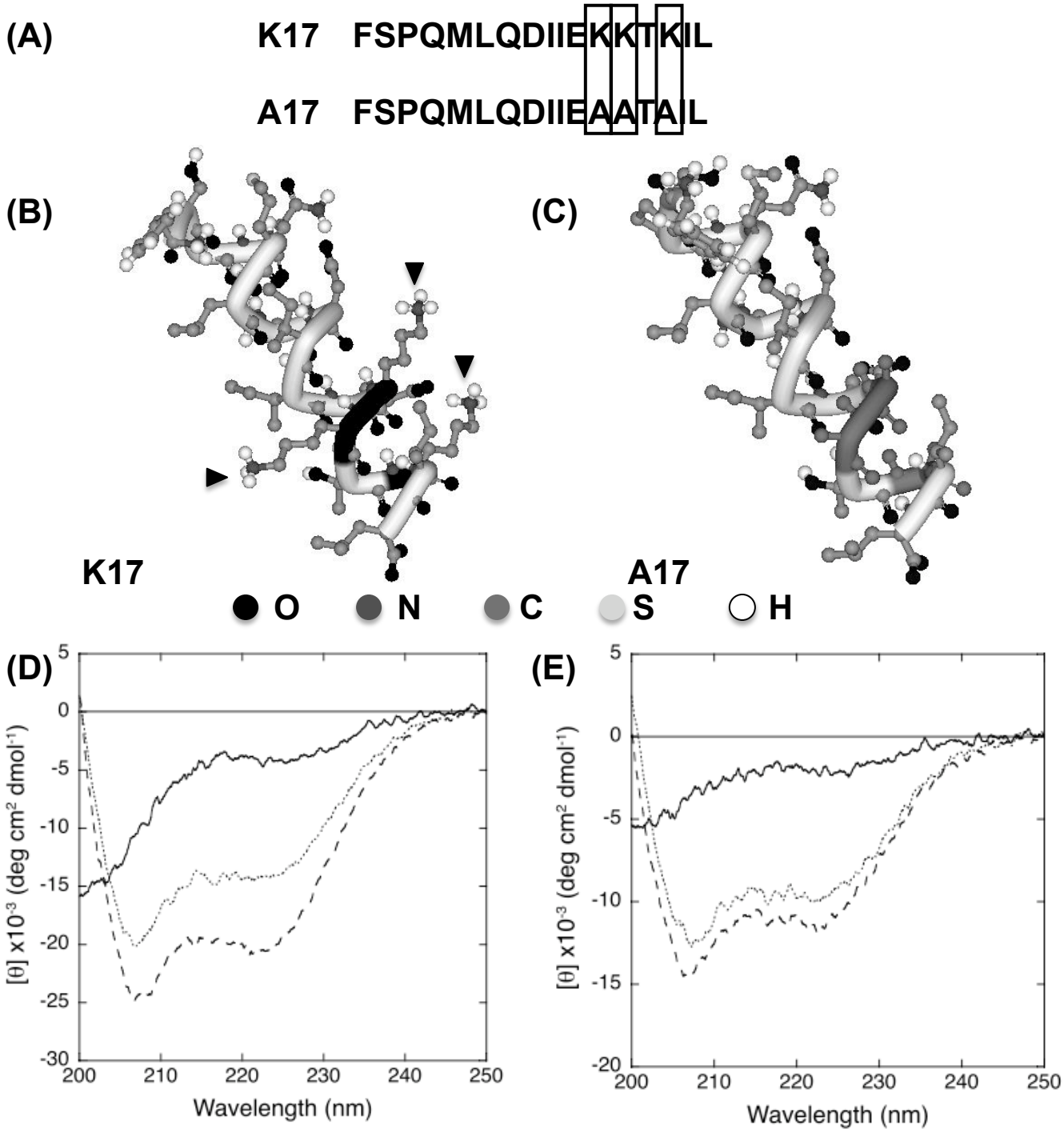

Figure 3 Secondary structures of the peptide derived from mBDLs sequence
(A) Amino acid sequences of K17 and the K17 analog, A17. Peptide sequences were based on the m*BDLs* exon 2 nucleotide sequence. (B and C) Estimated three-dimensional structures of K17 and A17 generated using PEP-FOLD software. The lowest energy model among the predicted structures is shown. Black color in K17 corresponds to main chain lysine residues (arrow heads). Estimated structure of A17, in which Lys-12, 13, and 15 of K17 were replaced with alanine. Gray color in A17 corresponds to main chain alanine residues. Representations were generated using Accelrys Discovery Studio software. (D and E) CD spectra of K17 (D) and A17 (E) under different conditions. The far-UV CD spectra of K17 (50 µg/ml) and A17 (100 µg/ml) was recorded in distilled water (solid line), 1% SDS (dotted line), or 50% TFE (dashed line).

Figure 4

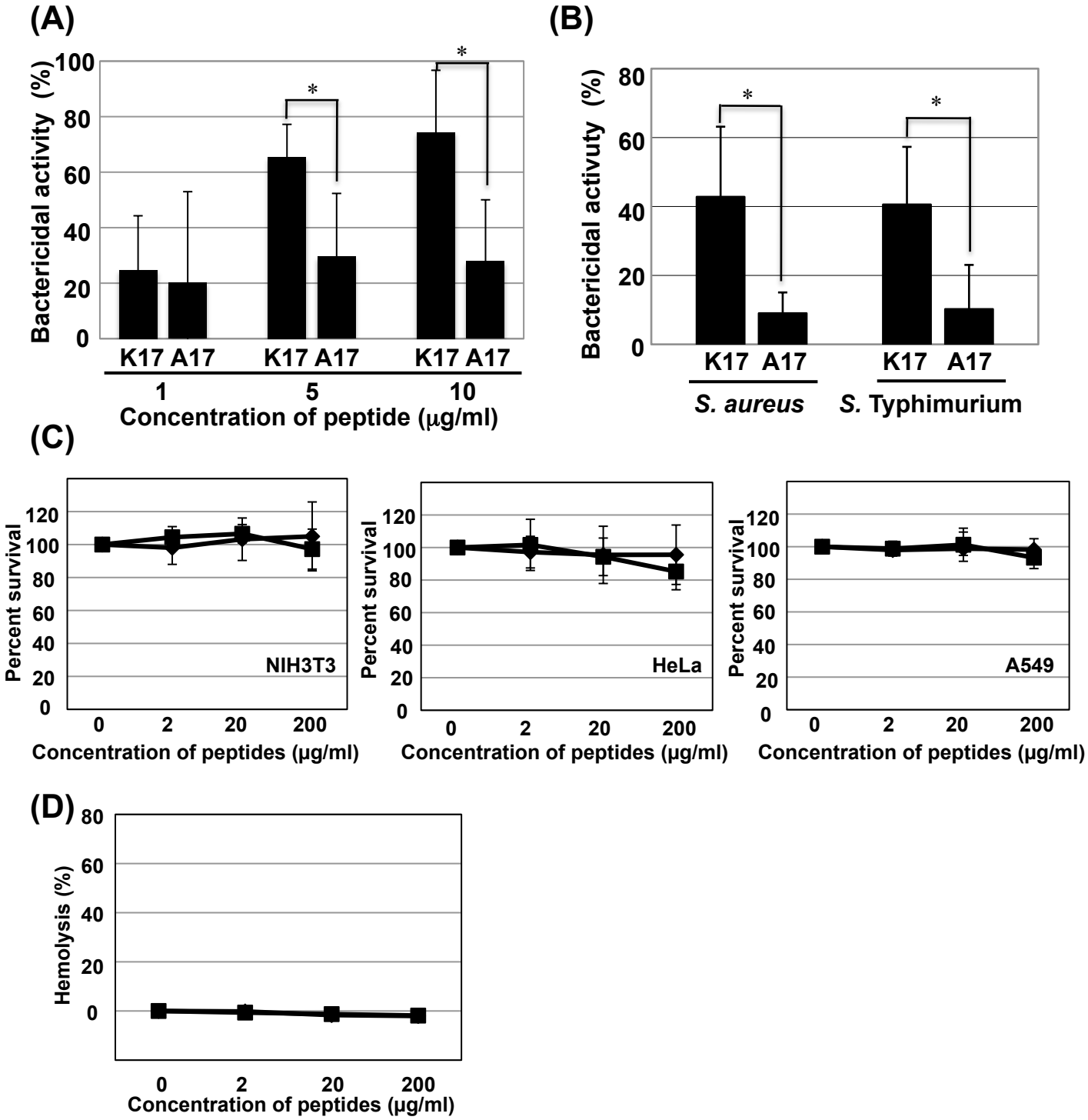

Figure 4 Functional analysis of K17
(A) Bactericidal activity of K17 and A17 against the defensin-sensitive *phoP*-strain of *S. typhimurium*. *, $p<0.05$. Mean CFUs were used to estimate survival. Data represents the percentage of bacteria killed in the peptide-treated sample as compared to the control (no peptide). (B) Bactericidal activity of K17 and A17 (5 μg/ml) against wild-type *S. typhimurium* and *S. aureus*. *, $p<0.05$. (C) Viability of NIH3T3, HeLa and A549 cells incubated with the indicated concentrations (2, 20, 200 μg/ml) of K17 (◆) and A17 (■). (D) Hemolytic activity of the indicated concentrations of K17 (◆) and A17 (■) in cultures of mouse erythrocytes.

[Chapter 2]

CXCR4 antagonist AMD3100 is a candidate for ATL therapeutic approach

(Inhibition of the SDF-1α-CXCR4 axis by the CXCR4 antagonist AMD3100 suppresses the migration of cultured cells from ATL patients and murine lymphoblastoid cells from HTLV-I Tax transgenic mice)

Introduction

Adult T−cell Leukemia (ATL) is a peripheral T-cell malignancy caused by infection by human T lymphotropic virus type I (HTLV-I). This hematological neoplasm develops in 1 to 5% of people infected with HTLV-I usually 2 to 4 decades after infection. A characteristic manifestation of ATL is extensive infiltration of leukemic cells into various organs, including lymph nodes, liver, spleen, lungs, and skin [20, 21]. Tissue infiltration likely reflects certain unique biological properties of the leukemic cells and although these are poorly understood they may be related to the expression and function of chemokines, chemokine receptor [22-26], adhesion molecules [27, 28], and resulting adhesive interactions with endothelial cells.

Chemokines are a group of structurally related cytokines that induce directed

migration of various leukocyte populations [29]. Chemokine receptors are coupled to heterotrimeric G proteins and induce cell movement toward a concentration gradient of the cognate chemokine ligand [30]. Chemokines are essential for the migration and tissue localization of various lymphocyte subpopulations expressing specific chemokine receptors. Human stromal-cell derived factor-1α (SDF-1α), also known as CXCL12, binds and signals solely though chemokine receptor CXCR4 [31]. CXCR4 is central to stem cell localization, serving as a chemoattractant for lymphocytes *in vitro* and *in vivo* [32]. In addition, a recent study demonstrated that the CXCR4 signal pathway may play a role in the metastasis of breast cancer cells by inducing chemotactic and invasive responses [33].

Human ATL cells have been shown to produce several chemokines, including macrophage inflammatory protein-1α (MIP-1α) [22], MIP-3α [23], MIP-1β [24], I-309 , thymus- and activation-regulated chemokine (TARC) [26], and macrophage-derived chemokine (MDC) [7],and express the chemokine receptors CCR4 [34], CCR5 [35], CCR7 [36] , and CCR9 [37], and it has been suggested that some of these may be involved in ATL cell migration and infiltration.

Recently, we have established a model of ATL by generating HTLV-I Tax transgenic mice with a restriction of transgene expression to developing thymocytes [38]. These mice developed aggressive leukemia and lymphoma with a characteristic histological phenotype showing extensive perivascular infiltration of leukemia cells into spleen, liver, kidney, lung, lymph nodes, and skins. Flow cytometric analyses demonstrated that the cells were CD4 and CD8 negative, but positive for both CD44 and cytoplasmic CD3

indicative of a thymus derived pre-T cell phenotype. Cells also expressed high levels of activation markers including CD25. Lymphomatous cells from these transgenic mice could reproduce identical disease after intraperitoneal injection into SCID mice. In this study, we have used the SCID mouse model to investigate molecular mechanisms associated with leukemic cell infiltration, and have focused on the chemotactic activity of the lymphomatous cells. We could demonstrate that not only primary murine lymphomatous cells but also human ATL cells exhibit specific chemotactic activity in response to SDF-1α and that this is associated with a specific interaction with CXCR4 and activation of ERK1/2 signaling. It could also be shown that AMD3100, a specific CXCR4 antagonist [39], markedly inhibited cell migration and phosphorylation of ERK1/2 by SDF-1α in both murine and human cells. In addition, AMD3100 inhibited infiltration of lymphomatous cells into liver and lung tissues in SCID mice. These results have identified a novel molecular mechanism associated with leukemic cell migration and provide a framework for designing new therapeutic strategies for the treatment of ATL.

Material and Methods

Cells

Tumor cells from spleens of HTLV-I *Tax*-transgenic mice, in which normal

splenocytes were replaced with lymphomatous cells, were isolated using a Lymphoprep kit (Axis-Shield ProC As, Oslo, Norway), and suspended in RPMI 1640 medium. Thereafter, lymphomatous cells (10^6/mL) were intraperitoneally injected into SCID mice. At 28 days after injection, tumor cells were again isolated from ascites and spleens of the injected SCID mice. The isolated tumor cells from SCID mice (primary murine lymphoblastoid [pML] cells) were harvested and kept frozen until use. The pML cells were cultured in RPMI 1640 medium supplemented with 10% fetal bovine serum (FBS; Hyclone, Logan, UT), antibiotics, and 2 mM L-glutamine, and maintained at 37°C in 5% CO_2 and investigated after 1 or 2 days in culture. As a control, T cells were isolated from spleens of C57BL/6 mice with a Pan T-cell Isolation Kit (Miltenyi Biotec Auburn, CA). Isolated control T cells were cultured in the same conditions as that of pML cells. Leukemic cells from ATL patients who were diagnosed on the basis of characteristic clinical features and laboratory findings were isolated by Ficoll-Hypaque gradient centrifugation and kept frozen until use. The cells were cultured for 2 days in RPMI 1640 medium supplemented with 20% FBS (Equitech-Bio, TX), antibiotics, 2 mM L-glutamine, and 1 ng/mL interleukin-2 (IL-2; Peprotech EC, London, UK), and maintained at 37°C in 5% CO_2. Isolated cells contained more than 90% leukemic cells at the time of analysis. The clinical and laboratory characteristics of ATL patients are shown in Table 1.

All animal experiments were approved by the Animal Care and Use Committee of the Hokkaido University School of Medicine and the Animal Care and Use Committee of the National Institute of Infectious Diseases. Tumor cells from ATL patients were

maintained in RPMI 1640 medium supplemented with 15% FBS (Equitech-Bio), penicillin G (50 U/mL), and streptomycin (50 μg/mL; Sigma-Aldrich, MO). Ethical permission for use of patient-derived cells and pathologic materials was approved by the Ethical Committee of the Oita University Faculty of Medicine and informed consent was obtained in accordance with the Declaration of Helsinki.

Antibodies and chemicals

Antibodies for phosphorylated forms of p44/42 mitogen-activated protein kinase, Akt, p38, phosphatidylinositol 3 kinase (PI3K), and IB, and total forms of p44/42 mitogen-activated protein kinase, Akt, and IB were obtained from Cell Signaling Technology (Danvers, MA). Anti–mouse/human CXC-chemokine receptor 4 (CXCR4/CD184) polyclonal antibody was purchased from eBioscience (San Diego, CA). Recombinant mouse thymus and activation regulated chemokine (TARC/CCL17), macrophage inflammatory protein 3 (MIP-3α/CCL20), recombinant murine and human stromal cell–derived factor-1 (SDF-1α/CXCL12) were purchased from Peprotech EC. Recombinant murine regulated on activation normal T expressed and secreted (RANTES/CCL5) and cutaneous T cell–attracting chemokine (CTACK/CCL27) were purchased from Acris Antibodies (Hiddenhausen, Germany). Recombinant mouse secondary lymphoid-tissue chemokine (SLC/Exodus-2) was purchased from Chemicon International (Temecula, CA). The CXCR4 antagonist, AMD3100 octahydrochloride, was purchased from Sigma-Aldrich. Mitogen-activated protein kinase (MEK) inhibitor, U0126, was purchased from Promega. All recombinant chemokines and antagonists

were dissolved in distilled water, and U0126 was dissolved in dimethyl sulfoxide. For immunohistochemical staining, monoclonal antihuman/mouse CXCL12/SDF-1α antibody (1:100; R&D Systems, Minneapolis, MN) was used.

Immunoblotting

pML cells were serum-starved for 2 h, and then lysates from 1 x 10^6 cells per sample were prepared after stimulation with SDF-1α (100 ng/mL) at the indicated time points. Protein content was determined using a Pierce BCA Protein Assay kit. Equal amounts of protein were separated by polyacrylamide gel electrophoresis and transferred onto polyvinylidene difluoride membranes (Immobilon-P; Millipore, Billerica, MA).

Chemotaxis assay

For cells from both ATL patients and pML cells, the migration efficiency of cells was assessed using 5-μm-pore Transwell filter membranes (Kurabo, Tokyo, Japan). For each membrane filter, 5 x 10^6 cells were cultured in 200 μL RPMI 1640 containing 0.5% bovine albumin. The membrane insert was placed in the well of the 24-well plate that contained 500 μL RPMI medium with murine recombinant chemokine the noted concentrations, and incubated at 37°C for 2.5 h. After removal of filter inserts, the number of cells that had migrated from the upper chamber to the lower well was counted using a hemocytometer viewed under a microscope. Chemokines used in the assays are as described in "Antibodies and chemicals." To examine the effect of antagonists on SDF-1α–induced chemotactic activity, cells were incubated with

antagonists for 1 h and then loaded in the upper chamber. Migrated cells were counted using a hemocytometer. The effect of SDF-1α on cell survival was measured by assays of viability at 24 or 48 h.

Flow cytometry

For quantification of cell-surface CXCR4 receptor expression, pML cells were incubated for 30 min with PE-conjugated rat anti–mouse-CD184/CXCR4 monoclonal antibody (x 20; BD Pharmingen, Heidelberg, Germany), or PE-anti–rat IgG2b (Beckman Coulter, Fullerton, CA) as an isotype control. The data obtained were analyzed using Flowjo software (Tree Star, Ashland, OR).

Reverse transcription and reverse-transcription–polymerase chain reaction

Total RNA was prepared from pML cells using TRIzol reagent (Gibco-BRL, Gaithersburg, MD). Total RNA (1 μg) was reverse-transcribed with Omniscript reverse transcriptase (Qiagen), according to the manufacturer's instructions. Polymerase chain reaction (PCR) was carried out in a volume of 20 μL; initial denaturation at 94°C for 2 min was followed by 30 cycles of 94°C for 15 sec, 58°C for 30 sec, and 68°C for 30 sec. As an internal control, β-*actin* was also amplified. The following primers were used: for *Tax*, 5'-AGGCAGATGAGAATGACCATGA-3' and 5'-TTTTCACTCCCAGGCTCTAAGC-3'; for SDF-1α, 5'-CACCGATCCACACAGAGTACTTG-3' and 5'-AGCCAACGTCAAGCATCTGA-3'; for β-actin, 5'-CTCCTTAATGTCAGCGATTTC-3' and

5'-CAGCCGTGCAACAA-TCTGAA-3'. PCR products were electrophoresed in agarose gel, and visualized using a UV illuminator.

Immunohistochemistry

Tissues were fixed in neutral-buffered formalin (Sigma-Aldrich), embedded in paraffin, sectioned, and stained with hematoxylin and eosin (H&E). For immunohistochemical staining, the sections were deparaffinized with xylene and dehydrated using decreasing concentrations of ethanol. Thereafter, sections were boiled in a pressure cooker for 2 min in 0.01 M citrate buffer (pH 6.0) for antigen retrieval. Mouse sections were incubated with 0.3% H_2O_2 in methanol at room temperature for 15 min to block endogenous peroxidase. After washing with PBS, sections were pretreated with blocking solution A (Histofine; Nichirei Biosciences, Tokyo, Japan) at room temperature for 60 min. The sections were sequentially incubated with primary antibody at 4°C overnight, with blocking solution B (Nichirei Biosciences) for 10 min, and with universal immunoperoxidase polymer (Nichirei Biosciences) for 10 min. The signal was visualized with diamino-3, 3'-diaminobenzidine. For human sections, slides were initially treated with peroxidase block solution (Dako, Carpenteria, CA) for 5 min, and incubated with 10% normal goat serum (Nichirei Biosciences) at room temperature for 60 min. The sections were incubated with primary antibody at 4°C overnight, and thereafter followed by incubation for 90 min with labeled polymer-HRP antimouse conjugation (Envision system; Dako) and color development using diamino-3, 3'-diaminobenzidine. Tumor cells from human ATL patients were stained by the Giemsa

method to confirm their morphology. To examine expression of SDF-1 in human tissues infiltrated by ATL cells, liver samples infiltrated by ATL cells from ATL cases (n = 5) were immunohistochemically examined.

AMD3100 in vivo treatment

SCID mice [6-week-old; nontreated (NT)] were inoculated intraperitoneally with AMD3100 pretreated (AMD^+) or NT pML cells (5×10^2, 5×10^3, and 5×10^4 cells/mice, n = 5 in each group). In AMD^+ group, the pML cells were incubated with 20 μg/mL AMD3100 in RPMI (0.3% fetal calf serum) at 37°C for 30 min as described previously [40]. The mice inoculated with AMD^+ pML cells were treated with 300 μg AMD3100 daily for 3 weeks (5 days per week) intraperitoneally (AMD-treated mice). The mice inoculated with NT pML cells were treated with PBS for 3 weeks (5 days per week) intraperitoneally (untreated mice). The mice were killed at 23 days after inoculation of pML cells. Genomic DNA of liver and lung tissues was extracted, and the copy numbers of *Tax* gene and *β-actin* gene were measured by quantitative real-time PCR using QuantiTect Probe PCR Kit (Qiagen). The relative copy number of *Tax* was represented by the ratio to the copy number of *β-actin* gene. The primers used for detection of *Tax* genome and *β-actin* gene were as follows: Tax forward: 5'-AGGCAGATGACAATGACCATGA -3', Tax reverse: 5'-TTTTCACTCCCAGGCTCTAAGC -3', Tax probe: 5'-FAM-CCCCAATATCCCCCGGG -TAMRA-3', and beta-actin forward: 5'-CACCGATCCACACAGAGTACTTG -3', β-actin reverse: 5'-

CAGTGCTGTCTGGTGGTACCA -3', and β-actin probe: 5'-FAM-CAGTAATCTCCTTCTGCATCCTGTCAGCAA -TAMRA-3'.

Statistics

Statistical comparisons between experimental groups were analyzed using the Student *t* test, and for all comparisons a *P* value less than $p<0.05$ was considered significant.

Results

Chemotactic response of primary murine lymphomatous (pML) cells to SDF-1α

Several studies have reported that human ATL cells exhibit chemotactic activity in response to the chemokines TARC, SLC, and RANTES [26, 29, 30]. I examined the chemotactic activity of pML cells in response to several cytokines and chemokines. Specifically, the pML cell migratory response to 6 different chemokines, TARC, MIP-3α, RANTES, SLC, CTACK, and SDF-1α was investigated using a chemotaxis chamber assay. It could be shown that pML cells had a marked, dose-dependent chemotactic response to SDF-1α (Figure 5A). The cells also showed a weak chemotactic response to TARC and SLC, which has been reported for human ATL cells [26, 29]. The migratory efficiencies of pML cells and control normal mouse T-cells in

response to SDF-1α were compared and it could be clearly shown that the migratory response of pML cells was markedly higher (Figure 5B).

I examined the effect of SDF-1α on survival of pML cells. SDF-1α had no effect on survival of pML cells after 24 and 48 h incubation. I also investigated the effect of NF-κB inhibitor (BAY65-1942), which induces apoptosis of pML cells at 24 h after incubation, to determine whether SDF-1α might reverse this. More than 80% of the pML cells were dead at 24 h after incubation with BAY65-1942, and it could be clearly shown that SDF-1α could not reverse the effect of the inhibitor and permit the survival of the pML cells (Figure 6).

Cell surface localization of CXCR4 in pML cells

Flow cytometry analysis was used to examine expression of CXCR4, which is the specific receptor for SDF-1α on pML cells, and it could be shown that CXCR4 was localized on the cell surface (Figure 7A). Chemokine binding to their cell surface receptors is known to lead to internalization of the receptor-ligand complex, with subsequent activation of intracellular signal cascades [41]. To investigate the effect of SDF-1α on CXCR4 expression, I analyzed CXCR4 localization after treatment with SDF-1α (100 ng/ml). It could be demonstrated that treatment with SDF-1α down regulated CXCR4 surface expression (Figure 7B). Total expression levels of CXCR4 protein were unaffected (Figure 7C), demonstrating that cell surface CXCR4 in pML cells was internalized upon exposure to SDF-1α.

Intracellular signal pathways regulated by SDF-1α/CXCR4 in pML cells

SDF-1α is known to activate the ERK1/2 pathway. ERK1/2 is a downstream effector of the MEK-dependent signaling cascade, and the MEK-ERK pathway is an important mediator of chemotaxis in many cell types [42, 43]. To confirm whether SDF-1α treatment activates the MEK-ERK pathway in pML cells, I initially examined phosphorylation of ERK1/2. Immunoblotting with phospho-ERK antibody revealed that SDF-1α treatment led to a rapid activation of ERK1/2 (Figure 7D), with phosphorylation of ERK1/2 evident within 1 min and peaking at 5 min after SDF-1α exposure. This was sustained at least until 120 min. No significant changes were observed in total ERK protein expression over this time period (Figure 7D). These results were consistent with a previous study in which SDF-1α was shown to promote internalization of CXCR4 and activation of ERK1/2 in multiple myeloma cells [44].

Phosphorylation of ERK1/2 was found to be abrogated by the MEK inhibitor U0126, even in the presence of SDF-1α (Figure 8A), and about 40% decrease in the migration of pML cells was observed in chemotaxis assays (Figure 8B). To further analyze CXCR4/SDF-1α-mediated intracellular signaling, I investigated whether SDF-1α activated other molecules downstream of CXCR4. In contrast to ERK1/2, phosphorylation of a number of others molecules, including PI3K, Akt, p38, and IκBα, was not significantly affected (Figure 7D). These results demonstrate that SDF-1α exclusively activates the MEK-ERK pathway in pML cells.

Effects of the CXCR4 antagonist AMD3100 in pML cells

I investigated the effect of the selective CXCR4 antagonist AMD3100 on chemotaxis and ERK1/2 signaling. As previously shown, CXCR4 surface expression was downregulated by SDF-1α treatment (100 ng/ml); however this inhibition was abrogated by AMD3100 treatment (25 μg/ml) (Figure 7E). Total levels of CXCR4 protein expression were unchanged by AMD3100 treatment (Figure 7F). I also examined whether AMD3100 affects phosphorylation of ERK1/2, and it could be demonstrated that phosphorylation was markedly decreased (Figures 7D and G). SDF-1α-induced migration activity of pML cells was assayed in the presence of AMD3100 and compared with untreated cells, and migration was found to be inhibited 79% and 91.2% in the presence of 0.25 and 1.25 μg/ml AMD3100, respectively (Figure 7H). These results show that AMD3100 inhibits the migration of pML cells in a dose-dependent manner by inhibiting the MEK-ERK pathway downstream of CXCR4-SDF-1α.

Chemotaxis of cells derived from ATL patients in response to SDF-1α

To determine whether the results of my mouse model accurately reflected human disease, I analysed chemotactic activity of leukemic cells from 6 ATL patients after short-term culture (2 days) in response to SDF-1α. Clinical and laboratory information relating to the patients is summarized in Table 1. Phenotypic analysis of the leukemic cells showed that all cell populations were CD4+/CD25+, and Giemsa staining clearly demonstrated typical features of ATL with cells having enlarged nuclei, often with lobulation, compared with normal peripheral blood lymphocytes (data not shown). All

of the ATL cells exhibited chemotaxis in response to SDF-1α treatment in a dose-dependent manner (Figure 9A). In addition, immunoblotting revealed that SDF-1α-induced phosphorylation of ERK1/2 occurred in 4 of the 6 ATL cases examined (Figure 9B); immnoblotting studies in the 2 remaining cases could not be carried out due to insufficient amounts of cell lysates. AMD3100 treatment of the human ATL cells strongly blocked phosphorylation of ERK1/2 (Figure 9B), and abrogated cell migration (Figure 9C). These results clearly demonstrate involvement of the SDF-1α/CXCR4-ERK pathway in human ATL cell migration, and the inhibitory potential of AMD3100.

SDF-1α expression in tissues

SDF-1α is constitutively expressed in numerous tissues in mice [45]. I confirmed expression of SDF-1α mRNA in various organs, including brain, heart, lung, liver, spleen, and kidney. However, I was unable to demonstrate a positive signal for SDF-1α mRNA expression in pML cells (Figure 10A). To examine the presence of SDF-1α protein, I used two different antibodies for tissue analysis, and could detect positive signals using a monoclonal anti-CXCL12/SDF-1α antibody. Weak immunopositive signals for SDF-1α protein were observed in epithelial cells of mouse liver hepatic ducts (Figures 10B and C); no positive signals were observed in control experiments which used normal mouse IgG instead of primary antibody (data not shown). In HTLV-I Tax transgenic mice, leukemic cell infiltration was readily observed in areas surrounding the SDF-1α-immunopositive hepatic ducts (Figures 10D and, E).

In ATL patients, SDF-1α-immunopositive signals were readily detected in the epithelial cells of hepatic ducts that were surrounded by infiltrating leukemic cells (Figures 10F and G). I also observed SDF-1α-immunostaining in epithelial cells of regenerative hepatic ducts in regions infiltrated by leukemic cells (Figures 10H and I). Infiltrating cells were also detected in the portal triad region, and again specifically around the hepatic ducts where epithelial cells were positive for SDF-1α (Figures 10F-I). I also performed immunostaining with anti-SDF-1α antibody of control disease free human liver samples, and immunopositive staining was also detected in hepatic duct epithelial cells (Figures 10J and K).

Inhibition of pML cell invasion by AMD3100 *in vivo*

I performed *in vivo* experiments to determine whether AMD3100 could inhibit leukemic cell invasion in SCID mice. The mice inoculated intraperitoneally with AMD3100 pretereated (AMD^+) or nontreated (NT) pML cells (5×10^2, 5×10^3, and 5×10^4 cells/mice, n=5 in each group). The mice inoculated with AMD^+ pML cells were treated with AMD3100 (AMD-treated mice), and control mice inoculated with NT pML cells were treated with PBS (untreated mice) for 3 weeks (5 times per week) through intraperitoneal injection. The mice were sacrificed at 23 days post pML cell inoculation. Invasion of pML cells containing the HTLV-I *Tax* gene into liver and lung tissues was examined using quantitative real-time PCR. The relative copy number of Tax was represented by the ratio to the copy number of β-actin (Figure 11). In the pML cells inoculated group (5×10^2), the *Tax* gene was not detected in the liver of either AMD-

treated or untreated mice mice (n=5, in each group), whereas *Tax* was exclusively detected in one lung tissue of 5 untreated mice (Figure 11). When the mice were inoculated with 5 x 10^3 pML cells, the ratio of *Tax* genome to *β-actin* gene was significantly inhibited in AMD-treated mice in both liver and lung tissues compared with untreated mice. Furthermore, *Tax* was detected in all of the untreated mice (n=5), whereas this was not detected in any of the AMD-treated mice (n=5, Figure 9). No significant differences were observed between AMD-treated and untreated mice (n=5, in each group) that were inoculated with 5 x 10^4 pML cells (Figure 9). Thus, CXCR4/SDF-1α plays a key role in migration of ATL cells *in vivo* and AMD3100 inhibits infiltration of pML cells into liver and lung. The results also show that the inhibitory effect of AMD3100 on tissue infiltration of pML cells is influenced by the numbers of inoculated pML cells.

Discussion

Patients with aggressive ATL characteristically display symptoms of leukemic cell infiltration in multiple organs including skin, bone marrow, spleen, liver, lung, and brain. However, the mechanisms of ATL cell infiltration are poorly understood. Chemokines are small secretory proteins that control migration and activation of leukocytes and other types of cells through interaction with a group of seven-transmembrane-domain G

protein-coupled receptors (GPCRs). It is known that chemokines may also promote cellular growth and survival and have been associated with metastasis in several malignancies. Specifically it has been shown that, breast cancer cells express CXCR4, and high concentrations of SDF-1α are typically present at metastatic sites of breast cancer [33]. The interaction between SDF-1α and CXCR4 has also been implicated in bone metastasis in prostate cancer [46].

Little is known about the role of G proteins and GPCRs in the life cycle and pathogenesis of HTLV-I. Studies have shown that CCR4 [29] and CCR7 [21] are frequently expressed in ATL cells, and chemokines, including MCP-1 [3], RANTES [30], MIP-1α [24], and SDF-1α [47] have been shown to modulate migration and tissue localization of HTLV-I-infected cells. In addition, expression of the HTLV-I regulatory protein Tax in immortalized T-cell lines has been shown to be involved the activation of the SDF-1α/CXCR4 pathway [48].

The present study has clearly demonstrated the cell surface expression of CXCR4 on leukemic cells, a specific chemotactic response to SDF-1α, and that cell migration is associated with MEK-ERK signaling. Following the interaction with SDF-1α**,** surface CXCR4 translocates to an intracellular compartment [41]. It has been demonstrated that the GPCR heteromultimerized with receptors of tyrosine kinases translocated to the endosome and promoted activation of endosomal Ras-ERK pathways in several cell types [49]. Thus, it is possible that the subcellular localization of CXCR4 in pML cells may also promote activation of additional signaling pathways, in addition to ERK 1/2, and this is currently under investigation.

My studies also demonstrated that the CXCR4 antagonist AMD3100 inhibited cell migration in response to SDF-1α. The MEK inhibitor U0126 was found to inhibit the chemotaxis of pML cells and also inhibited phosphorylation of ERK 1/2. In contrast, AMD3100 although significantly suppressing they chemotactic activity of pML cells, had less impact on the phosphorylation of ERK1/2 compared with U0126 (Figures 7G-H and Figure 8). These results suggest that phosphorylation of ERK 1/2 may also be regulated by other cellular factors. Indeed, it is likely that other signaling pathways and other processes are involved downstream of CXCR4. I also performed a Mouse Inflammatory Cytokine and Receptors Microarray analysis in which 113 key genes are involved, to determine the possible role of other chemokine receptors (SABiosciences, Frederick, MD). Using pML cells and pan T cells derived from B6 mice I could not observe any up-regulation of other chemokine receptors in pML cells. Thus although the SDF-1α /CXCR4 pathway appears to be uniquely important, it is almost certain that other pathways also contribute to leukemic cell invasion, including cell adhesion molecules [27, 28], matrix metalloproteinases [50], and other biomolecules [51]. Microarray data have been deposited to Gene Expression Omnibus (GEO) and can be found under accession numbers GSE17341, GSM433627, and GSM433628.

The results obtained from my previous and the present studies also confirm that my murine models do accurately reproduce human disease in that, in addition to developing the clinical and pathological features of ATL, I also demonstrate a dose-dependent promotion of chemotactic activity by SDF-1α, phosphorylation of ERK1/2, and an

AMD3100 inhibition of SDF-1α-induced ERK1/2 phosphorylation and migration in primary human ATL cells.

SDF-1α is released from fibroblasts and is ubiquitously expressed in many tissues, including liver, kidney, and lung [45]. I confirmed SDF-1α mRNA expression in range of mouse tissues (Figure 4A) and that expression of SDF-1α may be associated with invasion of leukemic cells both in the mouse model and human disease.

AMD3100 is currently being evaluated in a phase I trial using healthy volunteers [52], and in a phase 2 trial involving HIV-I-infected patients [53]. In addition this drug is considered to be a promising candidate for the treatment of other disorders in which SDF-1α/CXCR4 interactions may be important, including rheumatoid arthritis [54], breast cancer metastasis [55], atherosclerosis, and asthma [56]. I demonstrated that AMD3100 inhibited infiltration of pML cells into liver and lung tissues in SCID mice but that the inhibitory effect was influenced by the number of inoculated pML cells. These results imply that when a large number of leukemic cells are used in the inoculation this can overcome the inhibitory effect of AMD3100. This could be related to the levels of AMD3100 and may require more optimal dosing or to other unknown factors. This is currently under investigation but my results prove in principle the role of AMD3100 in preventing infiltration of leukemic cells and support the findings of my in vitro experiments. My studies also suggest that AMD3100 should be a considered as a candidate agent as part of combination therapy of ATL. It has been shown that a

combination of α interferon with retrovir can produce significant remission in certain ATL patients [57], and it is possible that the addition of AMD3100 could contribute to the efficacy of this combination. It is certainly likely that leukemic cell infiltration will involve other molecular mechanisms and as such combination therapy in the future would also include inhibitors of these processes. Clinical trials in my murine model and ultimately in human disease will ascertain whether CXCR4 antagonists and other agents will play a role and/or contribute to treatment efficacy in combination therapeutic approaches.

Summary

Adult T-cell leukemia (ATL) is a T-cell malignancy caused by HTLV-I, and presents as an aggressive leukemia with characteristic widespread leukemic cell infiltration into visceral organs and skin. The molecular mechanisms associated with leukemic cell infiltration are poorly understood. I have used mouse models of ATL to investigate the role of chemokines in this process. Transfer of splenic lymphomatous cells from transgenic to SCID mice reproduces a leukemia and lymphoma that is histologically identical to human disease. It could be shown that lymphomatous cells exhibit specific chemotactic activity in response to stromal-derived factor-1α (SDF-1α). Lymphomatous cells exhibited surface expression of CXCR4, the specific receptor of SDF-1α and

chemotaxis was associated with down regulation of CXCR4 expression and phosphorylation of intracellular ERK1/2. AMD3100, a CXCR4 antagonist, was found to inhibit both SDF-1α - induced migration and phosphorylation of ERK1/2. Investigation of cultured cells from human ATL patients revealed identical findings. Using the SCID mouse model, it could be demonstrated that AMD3100 inhibited infiltration of lymphomatous cells into liver and lung tissues *in vivo*. These results demonstrate the involvement of the SDF-1α/CXCR4 interaction as one mechanism of leukemic cell migration and this may provide a novel target as part of combination therapy for ATL.

Table 1 Patient characteristics

Case	date of collection	age/sex	Subtype at diagnosis	date of onset	WBC (/mm^3)	Atypical cells (%)*	LDH (IU/L) (normal range)***	Serum Ca (mg/dl) #	Infiltrated organs
1	2007/10/16	no data	chronic	no data	16800	80%	NE**	NE**	NE**
2	2000/6/9	70/F	chronic	2000/5/22	26250	34%	701 (212-410)	8.8	PB
3	2003/5/3	53/M	acute	2003/5/3	30870	69%	1426 (212-410)	normal	PB, S, superficial LN, LN in the abdominal cavity
4	2004/11/17	45/F	acute	2004/11/17	65540	83%	307 (119-229)	10.6	PB, S, L, Sp
5	1998/5/1	51/M	acute	1998/2/20	58820	88%	4979 (212-410)	10.1	PB, Sp
6	1996/11/8	36/M	acute	1996/11/6	37900	NE**	1349 (212-410)	9.15	PB, S, superficial LN, L, Sp

*** Atypical cells were morphologically diagnosed.**
**** not examined**
*****Normal range was changed in 2004.**
#normal range: 8.2-10.2 mg/dl
PB: peripheral blood, S: skin, L: liver, Sp: spleen, LN: lymph nodes

Figure 5

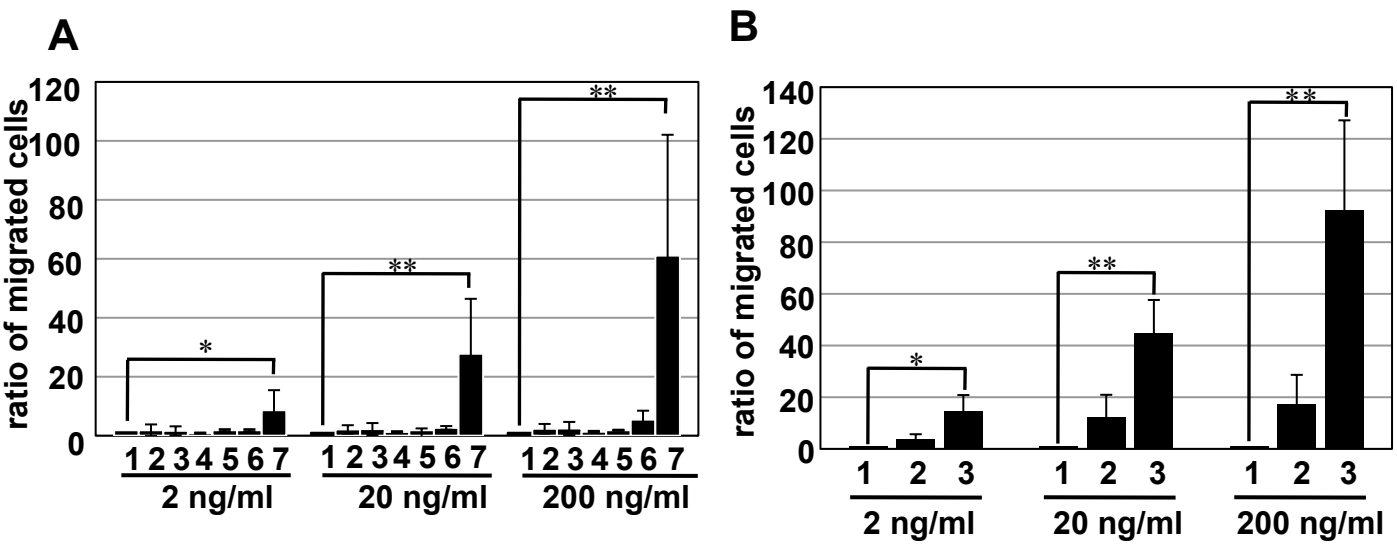

Figure 5 Chemotactic activity of pML cells in response to various chemokines.
(A) Chemotactic activity of pML cells in response to chemokines SDF-1α, MIP-3α, TARC, SLC, RANTES, and CTACK. Migration efficiency of pML cells was estimated using a Transwell assay in the presence of various concentrations (2, 20, and 200 ng/mL) of chemokines. The number of migrating pML cells was counted using a hemocytometer viewed under a microscope. The results are expressed as the fold number of the untreated control pML cells. The number below each bar corresponds to each chemokine: 1, control; 2, TARC; 3, MIP-3α; 4, RANTES; 5, CTACK; 6, SLC; and 7, SDF-1α. These results were confirmed by 3 independent experiments. The data are presented as mean values ± SD. *$P < .05$. **$P < .01$. (B) Chemotactic activity of pML cells and normal T cells. The number of migrating cells was measured as described for panel B in the presence of 0, 2, 20, and 200 ng/mL SDF-1. The results are expressed as the fold number of the normal T cells. These results were confirmed by 3 independent experiments. The data are presented as mean values ± SD. *$P < .05$; **$P < .01$.

Figure 6

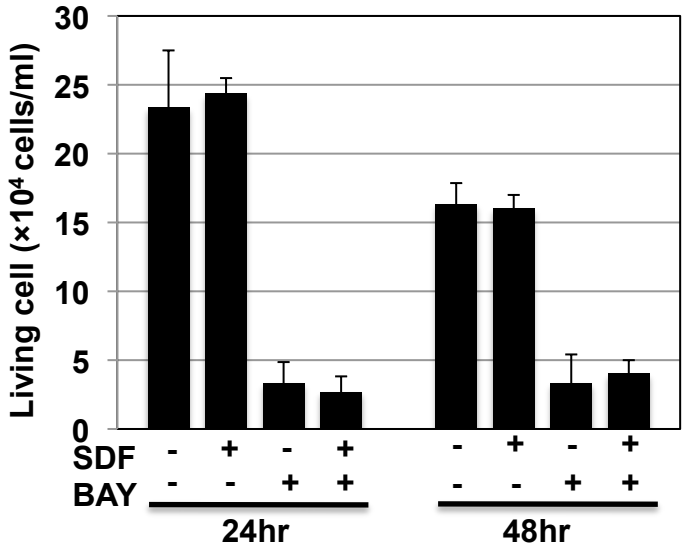

Figure 6 Effects of SDF-1α on survival of pML cells

We investigated the effect of SDF-1α on the survival of pML cells. After 24 hr culture, pML cells were treated with SDF-1α (200 ng/ml), NF-κB inhibitor (BAY65-1942, 10 μg/ml), or a combination of SDF-1α (200 ng/ml) and BAY65-1942 (10 μg/ml) for 24 h. At 24 h, the number of living cells was confirmed by trypan-blue staining. 30% of the cells were spontaneously dead after further incubation for 24 h in the presence or absence of SDF-1α. Thus there was no effect of SDF-1α on the survival of pML cells. More than 80% of the pML cells were dead at 24 h after incubation with BAY65-1942, and SDF-1α could not rescue the survival of the pML cells. Thus, SDF-1α does not play any role in the survival or reverse the effect of the NF-κB inhibitor.

Figure 7

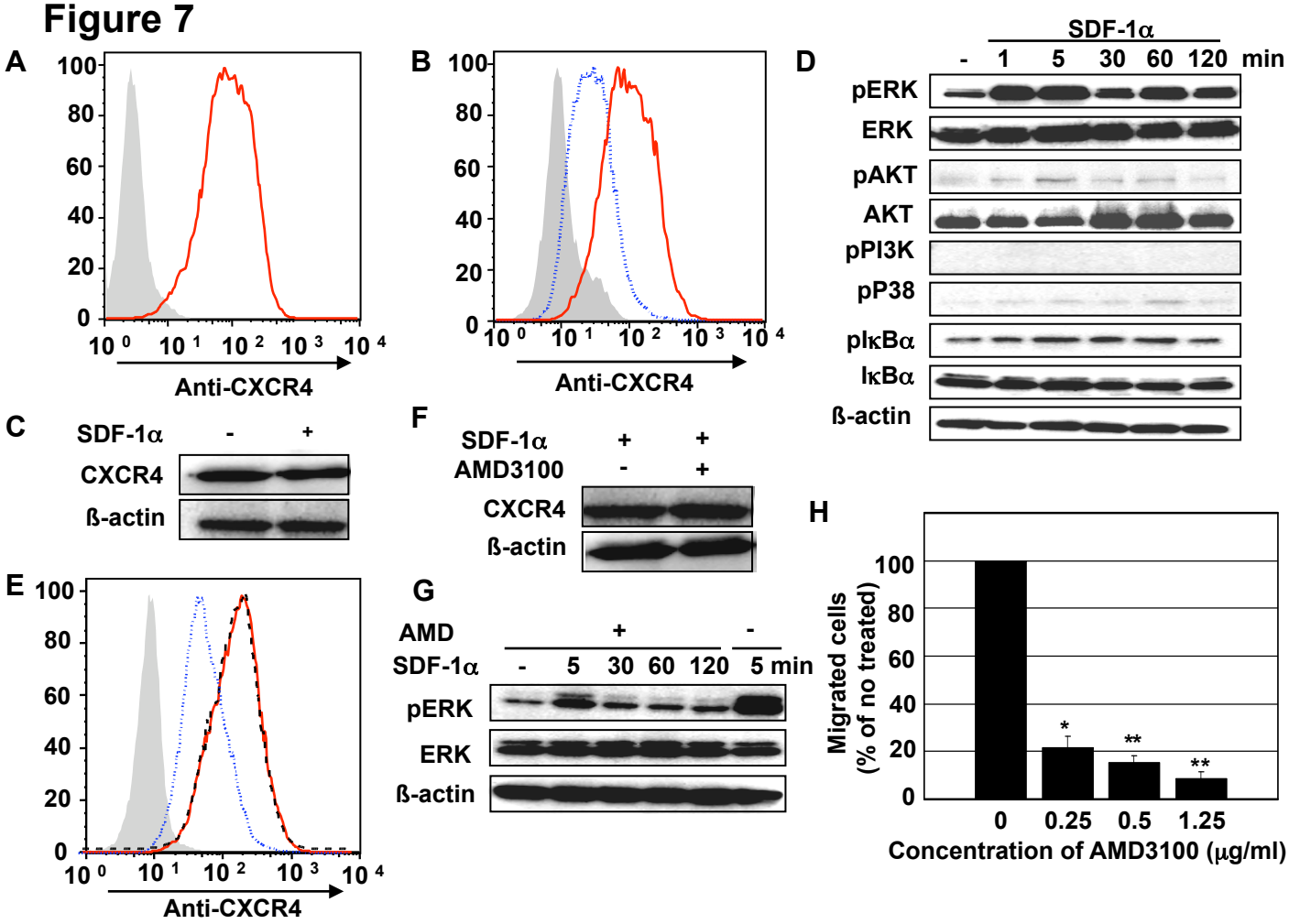

Figure 7 CXCR4 expression on the surface of pML cells and SDF-1α-induced CXCR4 translocation. **(A) Flow cytometry analysis of cell surface expression of CXCR4 in pML cells. CXCR4 was detected by incubating cells with PE-conjugated rat-anti-CXCR4 antibody. Red line represents CXCR4 expression, and gray area represents the result of staining with isotype-matched control antibody. (B) CXCR4 expression on pML cells surface. Cells were treated in the presence (blue dot line) or absence (red line) of 100 ng/ml SDF-1α. After a brief wash, cells were incubated with the same antibody as used in Figure 7A. The gray area represents staining with isotype-matched control antibody. (C) Total cellular protein level of CXCR4 in the presence (+) or absence (-) of SDF-1α (100 ng/ml) for 5 min. (D) SDF-1α-induced phosphorylation of ERK1/2 in pML cells. pML cells were treated prior to lysis with 100 ng/ml SDF-1α for the indicated time. Cell lysates were analyzed by immunoblotting analysis with anti-phospho-ERK, -total ERK, -phospho-AKT, -total AKT, -phospho-PI3K, -phospho-P38, -phospho-IκBα, -total IκBα or -β-actin antibodies. (E) Expression levels of cellular surface CXCR4 in pML cell after treatment with AMD3100. Cells were pretreated with 25 μg/ml AMD3100 for 1 h, and then stimulated with SDF-1α for 5 min (black dot line). Cells were also stimulated exclusively with SDF-1α (blue dot line) or were untreated (red line). The gray area represents staining with isotype-matched control antibody. (F) Expression of total CXCR4 protein with (+) or without (-) AMD3100 treatment. The lysates from treated cells were analyzed by immunoblotting with anti-mouse/human CXCR4 polyclonal antibody. (G) Phosphorylation of ERK1/2 in pML cells with or without AMD3100 treatment. After pretreatment with AMD3100 (25 μg/ml) for 1 h, cells were stimulated with SDF-1α for the indicated time (0, 5, 30, 60, and 120 min). The cellular lysates were analyzed by immunoblotting. In the lane at the right the cells received no AMD3100 treatment, but were stimulated with SDF-1α. (H) Migration assay of pML cells using AMD3100 at various concentrations (0, 0.25, 0.5, and 1.25 μg/ml). pML cells were preincubated for 60 min with AMD3100 at the indicated concentrations, and then subjected to the migration assay in the presence of 100 ng/ml SDF-1α. The data were presented as a relative ratio of migrating cells: the number of migrated cells in the presence of AMD3100/the number of non-treated cells. These results were confirmed by three independent experiments. The data are presented as mean values ± S.D.*, $P < 0.05$. **, $P < 0.01$.**

Figure 8

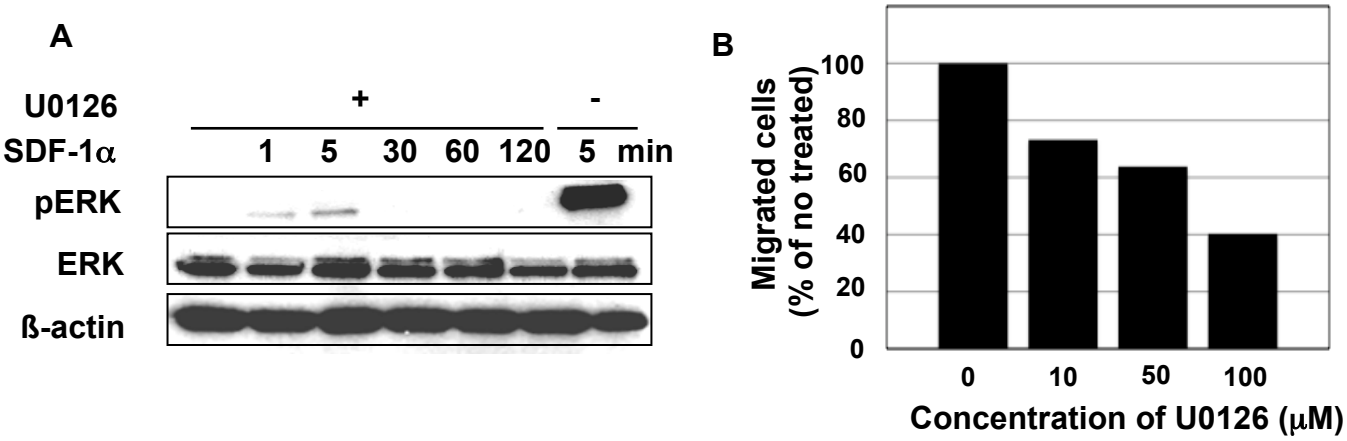

Figure 8 Effects of U0126 on pML cells
(A) pML cells were pretreated with U0126 (10 μM for 1 h), and exposed to SDF-1α for 0, 1, 5, 30, 60, and 120 min prior to lysis. In the lane at the right cells received no U0126 treatment and were stimulated with SDF-1α. (B) Migration assay of pML cells using U0126 at various concentrations (0, 10, 50, and 100 μM). pML cells were preincubated for 60 min with U126 at the indicated concentrations, and then subjected to the migration assay in the presence of 100 ng/ml SDF-1α. The number of the migrating cells was counted, and represented in the bar graph as a relative ratio of migrated to non-treated cells. Experiment was carried out two times and average of these results was shown.

Figure 9

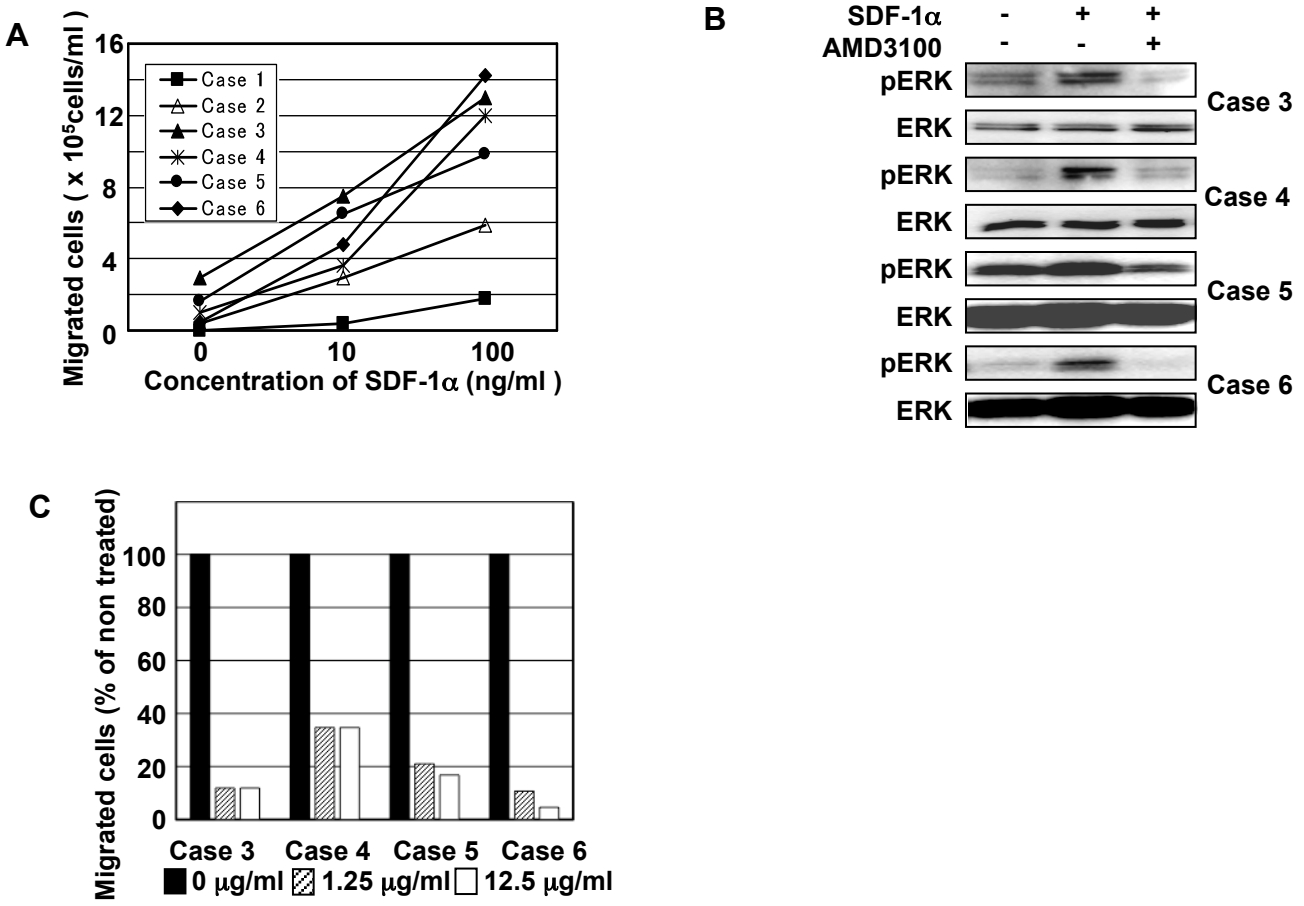

Figure 9 Chemotaxis of human ATL cells in response to SDF-1α.
(A) The migration assay of human ATL cells freshly prepared from frozen stocks of ATL patient's PBMCs and cultured for 2 days. Human ATL cells were also examined for chemotactic activity in response to SDF-1α, as described above, using recombinant human SDF-1α. After incubation with SDF-1α for 2.5 h, the number of the cells migrating to the lower chamber was counted using a hemocytometer. (B) Phosphorylation of ERK1/2 after stimulation with SDF-1α (100 ng/ml for 5 min) in human ATL cells with or without AMD3100 pretreatment (25 μg/ml for 1 h). (C) The inhibitory effect of AMD3100 on the migration of human ATL cells. Human ATL cells were preincubated for 60 min with the indicated concentrations of AMD3100, and then applied to the migration assay in the presence of 100 ng/ml SDF-1α. The number of the migrating cells was counted, and represented in the bar graph as a relative ratio of migrated to nontreated cells.

Figure 10

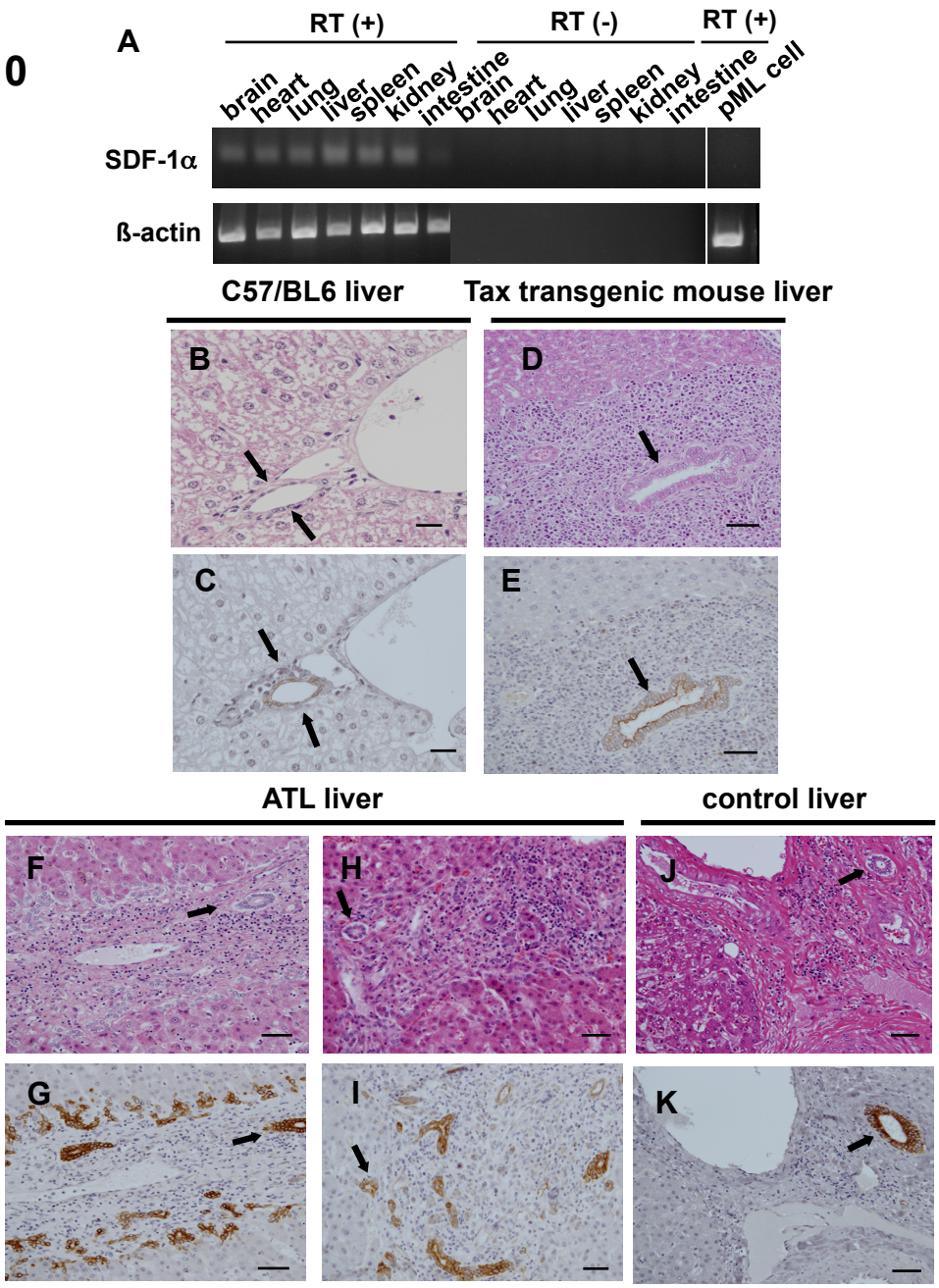

Figure 10 Tissue expression of SDF-1α.
(A) The expression levels of SDF-1α transcripts in various tissues of C57BL/6 mice, including brain, heart, lung, liver, spleen, kidney, and intestine with or without reverse transcriptase (RT) reaction. In the lane at the right the expression level of SDF-1α transcripts in pML cells was also examined. β-actin was used as an internal control. (B-K) Immunohistochemical analysis of SDF-1α protein. H&E staining (B and D) and immunostaining of SDF-1α (C and E) in bile ducts from a normal C57BL/6 mouse (B and C) and in a bile duct surrounded by infiltrating tumor cells from a HTLV-I Tax transgenic mouse (D and E). Black arrows indicate the same bile duct in serial sections for B and C, and D and E. Bars indicate (B and C) 20 μm, or (D and E) 50 μm. Immunohistochemical analysis of SDF-1α protein in liver bile ducts from ATL patients (F-I) and a patient without ATL (J and K). Serial sections of H&E stained liver from ATL patients (F and H) were examined with immnostaining using anti-SDF-1α antibody (G and I). Black arrows indicate the same bile duct in serial sections for F and G, and H and I. (J) Serial sections of H&E stained liver from a patient without ATL was also analyzed for SDF-1α expression (K). Black arrows indicate serial sections of the same bile ducts for J and K. Bars indicate 50 μm. Brown color indicates immunopositive reaction (C, E, G, I, K).

Figure 11

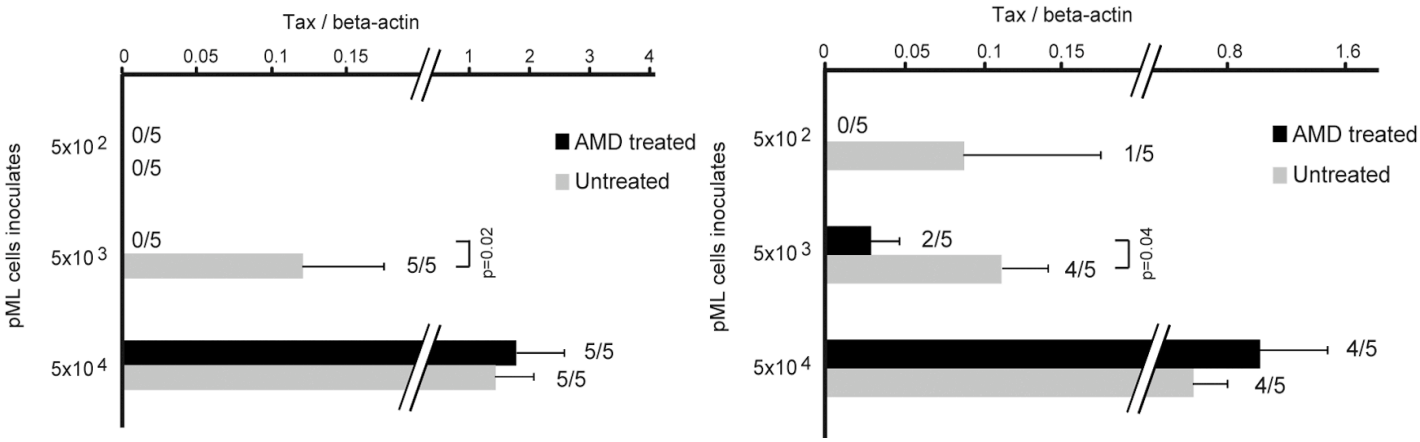

Figure 11 Inhibition of pML cell invasion by AMD3100 *in vivo*.
Infiltration of pML cells to the liver (A) and lung (B) was inhibited by AMD3100 treatment. SCID mice inoculated with pML cells (5 x 10^2, 5 x 10^3, and 5 x 10^4 cells/mice) were treated with either AMD3100 (AMD treated) or PBS (untreated) for 3 weeks (5 times per week) through intraperitoneal injection. Infiltration of pML cells which contain the HTLV-I Tax gene into liver and lung tissues was examined using quantitative real-time PCR. The relative copy number of *Tax* genome of the group (inoculated with 5 x 10^2, 5 x 10^3, and 5 x 10^4 of pML cells) was represented by the ratio to the copy number of β-actin in liver (A) and lung (B) tissues. The ratio of *Tax*-positive mice/total number of mice was represented on the right side of each bar.

General Conclusion

It is thought that the main strategies for infectious diseases are “prevention” and “treatment”. Epidemiological research and development of vaccine play a pivotal role in prevention of infectious diseases. Because it is difficult to achieve overcoming of infectious diseases only by preventive strategy, eradication of pathogens and symptomatic treatment are also important. In this study, I focused on host factors related to immunoreaction and chemoattraction against infection and attempted to obtain basic findings for development of therapeutic strategy against infection.

In the chapter I, I examined the efficacy of antimicrobial peptides (AMPs) against bacterial infection. AMPs play pivotal role in innate immunity which is non-specific and fast-acting defense system against infection and bind to bacterial membrane, resulting in bactericidal activity. For this non-specific defense activity, it is suggested that the emergence of AMPs–resistant bacteria rarely occur and AMPs may be useful for therapeutic strategy for infectious diseases.

I isolated a novel gene that is similar to mouse β–defensins and observed that location of this gene in genome and characteristics of gene structure are very common to that of β-defensins. Moreover, I predicted the region appropriate to the mature peptide of this gene, synthesized a small peptide based on this sequence (K17), and analyzed structure and function of the small peptide. This peptide has positive charge as same as known AMPs. Circular dichroism (CD) spectroscopy analysis of K17

demonstrates that K17 presents random coil conformation in aqueous solution, but adopts α-helical conformation in a membrane-mimicking environment. K17 exhibited bactericidal activity against *Salmonella enterica* serovar Typhimurium (Gram negative) and *Staphylococcus aureus* (Gram positive), but it was not cytotoxic in cultures of mammalian cells or hemolytic in cultures of erythrocytes. From these results, the peptide that I synthesized in this study may be a candidate therapeutic for the treatment of infectious disesases.

In the chapter II, I aimed at the host response occurred after the development of Adult T-cell Leukemia (ATL). ATL is the T-cell malignancy caused by Human T-cell leukemia virus type-I (HTLV-I) that belongs to retrovirus. Because there is no effective ATL therapy, the development of therapy is needed. A characteristic manifestation of ATL is extensive infiltration of leukemic cells into various organs, including lymph nodes, liver, spleen, lungs, and skin. The molecular mechanisms associated with ATL cell infiltration are poorly understood. Therefore, the investigation of the infiltration mechanism may be important for development of ATL therapy. Because tumor cells are attracted to several tissues by chemokine exist in that tissue, I examined the response of ATL cells to several chemokines and found that ATL cells show markedly response to stromal-cell derived factor-1α (SDF-1α). AMD3100, the antagonist against CXCR4 that is receptor for SDF-1α, suppressed the responsibility and the infiltration of ATL cells to tissues in mouse model. These results suggest the SDF-1α/CXCR4 interaction involve in leukemic cell migration and this pathway may become a novel candidate target for

ATL therapy.

It is clinically important to develop the therapeutic strategy for overcoming of infectious disease. In this study, a bactericidal strategy by AMPs and inhibition of infiltration of ATL cells by their receptor antagonists were demonstrated. It is suggested that obtained results lead to development of therapeutic strategy for infectious disease.

Abstract in Japanese (要旨)

抗菌ペプチドと受容体拮抗剤を用いた感染症治療法の開発

感染症対策の柱は「予防」と「治療」であり、予防対策の中心は疫学調査とワクチン開発である。しかし予防対策のみでは感染症の克服は困難であり、感染後の病原体の排除や、病態の改善を目的とした治療も重要である。本研究は感染応答に関与する宿主因子に着眼して、感染に対する治療法開発の基礎的知見を得ることを目的とした。

第 1 章では、宿主の免疫機構を担う自然免疫に着眼した。自然免疫は病原体が侵入した際に最初に働く非特異的な免疫機構である。自然免疫因子に属する抗菌ペプチドは病原体の膜に結合して破壊することで抗菌活性を示す。この結合は非特異的であるので広範囲の病原体に作用し、耐性が獲得されにくいという利点がある。その為、感染症の治療への応用の可能性が提唱され、注目されている。

本研究では、抗菌ペプチドである defensin と相同性が高い新規の遺伝子を単離し、この遺伝子がゲノム上の位置や構造の点でも β-defensin と相同性が高いことを明らかにした。次に、この新規遺伝子のアミノ酸配列を基に mature peptide 相当部分を予測し、17 残基からなるペプチドを合成し、その構造と機能を解析した。本ペプチドは既知の抗菌ペプチドと同様に正の電荷を有しており、Circular dichroism (CD)スペクトルを用いた構造解析の結果から、水溶状態ではランダムコイル構造をとるが、負電荷界面活性剤による変性やアルコール変性を起こし

た膜の模倣状態下では α-helix 構造をとるという抗菌ペプチドに共通する特徴を有していた。また本ペプチドは、哺乳類由来細胞には細胞毒性を示さない濃度で抗菌活性を示した。これらの結果から、本研究で合成したペプチドは感染症治療薬として応用できる可能性があると考えられた。

第 2 章では、未だ治療法が確立されていない感染症である Adult T-cell Leukemia (ATL)発症後の宿主応答に着眼した。ATL はレトロウイルスに属する T 細胞指向性のウイルス、(Human T-cell Leukemia Virus Type-I ; HTLV-I)によって惹起される T 細胞性の白血病である。発症後の予後は不良であり治療法の確立が急務である。腫瘍細胞の全身への浸潤の結果生じる多臓器不全が死因となる為に、腫瘍細胞の浸潤のメカニズムの解明は ATL の治療法を開発する上で必要である。腫瘍細胞は生体内のケモカインにより臓器へと誘引される。本研究は ATL 腫瘍細胞の種々のケモカインに対する応答性を in vitro において検討した結果、Stromal-cell Derived Factor-1α (SDF-1α)に対する応答性が有意に高いことを明らかにした。SDF-1α の受容体である CXCR4 に対するアンタゴニスト(AMD3100)はその応答性を抑制し、マウスを用いた実験においても腫瘍細胞の組織浸潤を抑制した。以上の結果から本化合物が ATL の治療薬の候補となることが示された。

実際の臨床現場では感染後や感染症発症後に治療対策をとることが多く、治療法の開発は感染症の克服において重要な課題である。本研究で示した抗菌ペプチドを用いた病原体の排除や、化合物を用いた感染症の病態改善を目指す試みは感染症の治療法の開発につながり、感染症の克服に大きく貢献できると考えられる。

Acknowledgement

I would like to express sincere gratitude to Professor Hirofumi Sawa, Department of Molecular Pathobiology, Research Center for Zoonosis Control, Hokkaido University, for supporting me throughout the experimental work and the preparation of this thesis. I am also gratitude to Dr. Hideki Hasegawa, National Institute of Infectious Diseases for supporting me throughout the experimental work.

I would like to express my great thanks to Associate professor Takashi Kimura (Department of Molecular Pathobiology), Research Center for Zoonosis Control, Hokkaido university for discussion and to Professor Tokiyoshi Ayabe, Faculty of Advanced Life Science, Innate immunity Laboratory, Hokkaido University and Associate Professor Naoki Sakai, Faculty of Advanced Life Science, Innate Immunity Laboratory, Hokkaido University, for discussion and technical support for bacterial experiment and CD spectroscopy analysis.

I am also deeply grateful to Professor Chihiro Sugimoto, Department of Collaboration and Education, Research Center for Zoonosis Control, Hokkaido University, Professor Takashi Umemura, Laboratory of Comparative Pathology, Department of Veterinary Clinical Sciences, Graduate School of Veterinary Medicine, Hokkaido University, and Professor Kazuhiko Ohashi, Laboratory of Infectious Diseases, department of Diseases Control, Graduate School of Veterinary Medicine, Hokkaido University for reviewing the manuscript, valuable advices, and suggestions.

I express my appreciation to all members of the Department of Molecular

Pathobiology, Research Center for Zoonosis Control, Hokkaido University for their encouragement and excellent technical assistance.

Finally, thanks are also due to my family and friends supporting me all through the time.

Reference

[1] K. Brogden, Antimicrobial peptides: pore formers or metabolic inhibitors in bacteria., Nat Rev Microbiol 3 (2005) 238-250.

[2] D. Andreu, L. Rivas, Animal antimicrobial peptides: an overview., Biopolymers 47 (1998) 415-433.

[3] J. Maupetit, P. Derreumaux, P. Tuffery, PEP-FOLD: an online resource for de novo peptide structure prediction., Nucleic Acids Res 37 (2009) W498-503.

[4] Ayabe T., Satchell D., Wilson C., Parks W., Selsted M. and Ouellette A. Secretion of microbicidal alpha-defensins by intestinal Paneth cells in response to bacteria., Nat Immunol 1 (2000), 113-8.

[5] J. Stalker, B. Gibbins, P. Meidl, J. Smith, W. Spooner, H. Hotz, A. Cox, The Ensembl Web site: mechanics of a genome browser., Genome Res 14 (2004) 951-955.

[6] R. Bals, X. Wang, R. Meegalla, S. Wattler, D. Weiner, M. Nehls, J. Wilson, Mouse beta-defensin 3 is an inducible antimicrobial peptide expressed in the epithelia of multiple organs., Infect Immun 67 (1999) 3542-3547.

[7] R. Lehrer, T. Ganz, Defensins of vertebrate animals., Curr Opin Immunol 14 (2002) 96-102.

[8] G. Morrison, C. Semple, F. Kilanowski, R. Hill and J. Dorin, Signal sequence conservation and mature peptide divergence within subgroups of the murine beta-defensin gene family, *Mol. Biol. Evol.* **20** (2003), pp. 460–470.

[9] A. Maxwell, G. Morrison and J. Dorin, Rapid sequence divergence in mammalian beta-defensins by adaptive evolution, *Mol. Immunol.* **40** (2003), pp. 413–421.

[10] G. Wang, X. Li, Z. Wang, APD2: the updated antimicrobial peptide database and its application in peptide design., Nucleic Acids Res 37 (2009) D933-937.

[11] H. Jia, S. Wowk, B. Schutte, S. Lee, A. Vivado, B. Tack, C. Bevins, P.J. McCray, A novel murine beta -defensin expressed in tongue, esophagus, and trachea., J Biol Chem 275 (2000) 33314-33320.

[12] G. Morrison, M. Rolfe, F. Kilanowski, S. Cross, J. Dorin, Identification and characterization of a novel murine beta-defensin-related gene., Mamm Genome 13 (2002) 445-451.

[13] G. Diamond, D. Jones, C. Bevins, Airway epithelial cells are the site of expression of a mammalian antimicrobial peptide gene., Proc Natl Acad Sci U S A 90 (1993) 4596-4600.

[14] Y. Tsutsumi-Ishii, I. Nagaoka, NF-kappa B-mediated transcriptional regulation of human beta-defensin-2 gene following lipopolysaccharide stimulation., J Leukoc Biol 71 (2002) 154-162.

[15] A. Tossi, C. Tarantino, D. Romeo, Design of synthetic antimicrobial peptides based on sequence analogy and amphipathicity., Eur J Biochem 250 (1997) 549-558.

[16] G. Saberwal, R. Nagaraj, Cell-lytic and antibacterial peptides that act by perturbing the barrier function of membranes: facets of their conformational features, structure-function correlations and membrane-perturbing abilities., Biochim Biophys Acta 1197 (1994) 109-131.

[17] S. Shin, J. Kang, S. Jang, Y. Kim, K. Kim, K. Hahm, Effects of the hinge region of cecropin A (1-8)-magainin 2 (1-12), a synthetic antimicrobial peptide, on liposomes, bacterial and tumor cells., Biochim Biophys Acta 1463 (2000) 209-218.

[18] M. Dathe, T. Wieprecht, Structural features of helical antimicrobial peptides: their potential to modulate activity on model membranes and biological cells., Biochim Biophys Acta 1462 (1999) 71-87.

[19] S. Shin, S. Lee, S. Yang, E. Park, D. Lee, M. Lee, S. Eom, W. Song, Y. Kim, K. Hahm, J. Kim, Antibacterial, antitumor and hemolytic activities of alpha-helical antibiotic peptide, P18 and its analogs., J Pept Res 58 (2001) 504-514.

[20] T. Uchiyama, Human T cell leukemia virus type I (HTLV-I) and human diseases., Annu Rev Immunol 15 (1997) 15-37.

[21] M. Matsuoka, Human T-cell leukemia virus type I and adult T-cell leukemia., Oncogene 22 (2003) 5131-5140.

[22] N. Mori, A. Ueda, S. Ikeda, Y. Yamasaki, Y. Yamada, M. Tomonaga, S. Morikawa, R. Geleziunas, T. Yoshimura, N. Yamamoto, Human T-cell leukemia virus type I tax activates transcription of the human monocyte chemoattractant protein-1

gene through two nuclear factor-kappaB sites., Cancer Res 60 (2000) 4939-4945.

[23] Y. Imaizumi, S. Sugita, K. Yamamoto, D. Imanishi, T. Kohno, M. Tomonaga, T. Matsuyama, Human T cell leukemia virus type-I Tax activates human macrophage inflammatory protein-3 alpha/CCL20 gene transcription via the NF-kappa B pathway., Int Immunol 14 (2002) 147-155.

[24] Y. Tanaka, S. Mine, C. Figdor, A. Wake, H. Hirano, J. Tsukada, M. Aso, K. Fujii, K. Saito, Y. van Kooyk, S. Eto, Constitutive chemokine production results in activation of leukocyte function-associated antigen-1 on adult T-cell leukemia cells., Blood 91 (1998) 3909-3919.

[25] T. Ruckes, D. Saul, J. Van Snick, O. Hermine, R. Grassmann, Autocrine antiapoptotic stimulation of cultured adult T-cell leukemia cells by overexpression of the chemokine I-309., Blood 98 (2001) 1150-1159.

[26] T. Shimauchi, S. Imai, R. Hino, Y. Tokura, Production of thymus and activation-regulated chemokine and macrophage-derived chemokine by CCR4+ adult T-cell leukemia cells., Clin Cancer Res 11 (2005) 2427-2435.

[27] T. Ishikawa, A. Imura, K. Tanaka, H. Shirane, M. Okuma, T. Uchiyama, E-selectin and vascular cell adhesion molecule-1 mediate adult T-cell leukemia cell adhesion to endothelial cells., Blood 82 (1993) 1590-1598.

[28] M. Tatewaki, K. Yamaguchi, M. Matsuoka, T. Ishii, M. Miyasaka, S. Mori, K. Takatsuki, T. Watanabe, Constitutive overexpression of the L-selectin gene in

fresh leukemic cells of adult T-cell leukemia that can be transactivated by human T-cell lymphotropic virus type 1 Tax., Blood 86 (1995) 3109-3117.

[29] D. Campbell, C. Kim, E. Butcher, Chemokines in the systemic organization of immunity., Immunol Rev 195 (2003) 58-71.

[30] O. Yoshie, T. Imai, H. Nomiyama, Chemokines in immunity., Adv Immunol 78 (2001) 57-110.

[31] T. Nagasawa, T. Nakajima, K. Tachibana, H. Iizasa, C. Bleul, O. Yoshie, K. Matsushima, N. Yoshida, T. Springer, T. Kishimoto, Molecular cloning and characterization of a murine pre-B-cell growth-stimulating factor/stromal cell-derived factor 1 receptor, a murine homolog of the human immunodeficiency virus 1 entry coreceptor fusin., Proc Natl Acad Sci U S A 93 (1996) 14726-14729.

[32] CC. Bleul, RC. Fuhlbrigge, JM.Casasnovas, A. Aiuti , TA. Springer. A highly efficacious lymphocyte chemoattractant, stromal cell-derived factor 1 (SDF-1). J Exp Med 184 (1996)1101–1109.

[33] B. Lee, T. Lee, S. Avraham, H. Avraham, Involvement of the chemokine receptor CXCR4 and its ligand stromal cell-derived factor 1alpha in breast cancer cell migration through human brain microvascular endothelial cells., Mol Cancer Res 2 (2004) 327-338.

[34] O. Yoshie, R. Fujisawa, T. Nakayama, H. Harasawa, H. Tago, D. Izawa, K. Hieshima, Y. Tatsumi, K. Matsushima, H. Hasegawa, A. Kanamaru, S. Kamihira, Y. Yamada, Frequent expression of CCR4 in adult T-cell leukemia

and human T-cell leukemia virus type 1-transformed T cells., Blood 99 (2002) 1505-1511.

[35] N. Mori, A. Krensky, K. Ohshima, M. Tomita, T. Matsuda, T. Ohta, Y. Yamada, M. Tomonaga, S. Ikeda, N. Yamamoto, Elevated expression of CCL5/RANTES in adult T-cell leukemia cells: possible transactivation of the CCL5 gene by human T-cell leukemia virus type I tax., Int J Cancer 111 (2004) 548-557.

[36] H. Hasegawa, T. Nomura, M. Kohno, N. Tateishi, Y. Suzuki, N. Maeda, R. Fujisawa, O. Yoshie, S. Fujita, Increased chemokine receptor CCR7/EBI1 expression enhances the infiltration of lymphoid organs by adult T-cell leukemia cells., Blood 95 (2000) 30-38.

[37] D. Nagakubo, Z. Jin, K. Hieshima, T. Nakayama, A. Shirakawa, Y. Tanaka, H. Hasegawa, T. Hayashi, K. Tsukasaki, Y. Yamada, O. Yoshie, Expression of CCR9 in HTLV-1+ T cells and ATL cells expressing Tax., Int J Cancer 120 (2007) 1591-1597.

[38] H. Hasegawa, H. Sawa, M. Lewis, Y. Orba, N. Sheehy, Y. Yamamoto, T. Ichinohe, Y. Tsunetsugu-Yokota, H. Katano, H. Takahashi, J. Matsuda, T. Sata, T. Kurata, K. Nagashima, W. Hall, Thymus-derived leukemia-lymphoma in mice transgenic for the Tax gene of human T-lymphotropic virus type I., Nat Med 12 (2006) 466-472.

[39] S. Hatse, K. Princen, K. Vermeire, L. Gerlach, M. Rosenkilde, T. Schwartz, G. Bridger, E. De Clercq, D. Schols, Mutations at the CXCR4 interaction sites for

AMD3100 influence anti-CXCR4 antibody binding and HIV-1 entry., FEBS Lett 546 (2003) 300-306.

[40] A. Colmone, M. Amorim, A. Pontier, S. Wang, E. Jablonski, D. Sipkins, Leukemic cells create bone marrow niches that disrupt the behavior of normal hematopoietic progenitor cells., Science 322 (2008) 1861-1865.

[41] N. Neel, E. Schutyser, J. Sai, G. Fan, A. Richmond, Chemokine receptor internalization and intracellular trafficking., Cytokine Growth Factor Rev 16 (2005) 637-658.

[42] R. Ganju, S. Brubaker, J. Meyer, P. Dutt, Y. Yang, S. Qin, W. Newman, J. Groopman, The alpha-chemokine, stromal cell-derived factor-1alpha, binds to the transmembrane G-protein-coupled CXCR-4 receptor and activates multiple signal transduction pathways., J Biol Chem 273 (1998) 23169-23175.

[43] SB. Peng, V. Peek , Y. Zhai , et al. Akt activation, but not extracellular signal-regulated kinase activation, is required for SDF-1alpha/CXCR4-mediated migration of epitheloid carcinoma cells. Mol Cancer Res 3 (2005) 227–236.

[44] Y. Alsayed, H. Ngo, J. Runnels , et al. Mechanisms of regulation of CXCR4/SDF-1 (CXCL12)-dependent migration and homing in multiple myeloma. Blood 7 (2007) 2708–2717

[45] K. Tashiro, H. Tada, R. Heilker, M. Shirozu, T. Nakano, T. Honjo, Signal sequence trap: a cloning strategy for secreted proteins and type I membrane proteins., Science 261 (1993) 600-603.

[46] P. Kukreja, A. Abdel-Mageed, D. Mondal, K. Liu, K. Agrawal, Up-regulation of CXCR4 expression in PC-3 cells by stromal-derived factor-1alpha (CXCL12) increases endothelial adhesion and transendothelial migration: role of MEK/ERK signaling pathway-dependent NF-kappaB activation., Cancer Res 65 (2005) 9891-9898.

[47] M. Moriuchi , H. Moriuchi , AS. Fauci. HTLV type I Tax activation of the CXCR4 promoter by association with nuclear respiratory factor 1. AIDS Res Hum Retroviruses15 (1999) 821–827.

[48] J. Twizere, J. Springael, M. Boxus, A. Burny, F. Dequiedt, J. Dewulf, J. Duchateau, D. Portetelle, P. Urbain, C. Van Lint, P. Green, R. Mahieux, M. Parmentier, L. Willems, R. Kettmann, Human T-cell leukemia virus type-1 Tax oncoprotein regulates G-protein signaling., Blood 109 (2007) 1051-1060.

[49] A. Mor, M. Philips, Compartmentalized Ras/MAPK signaling., Annu Rev Immunol 24 (2006) 771-800.

[50] N. Mori, H. Sato, T. Hayashibara, M. Senba, T. Hayashi, Y. Yamada, S. Kamihira, S. Ikeda, Y. Yamasaki, S. Morikawa, M. Tomonaga, R. Geleziunas, N. Yamamoto, Human T-cell leukemia virus type I Tax transactivates the matrix metalloproteinase-9 gene: potential role in mediating adult T-cell leukemia invasiveness., Blood 99 (2002) 1341-1349.

[51] T. Hayashibara, Y. Yamada, T. Miyanishi, H. Mori, T. Joh, T. Maeda, N. Mori, T. Maita, S. Kamihira, M. Tomonaga, Vascular endothelial growth factor and

cellular chemotaxis: a possible autocrine pathway in adult T-cell leukemia cell invasion., Clin Cancer Res 7 (2001) 2719-2726.

[52] C. Hendrix, C. Flexner, R. MacFarland, C. Giandomenico, E. Fuchs, E. Redpath, G. Bridger, G. Henson, Pharmacokinetics and safety of AMD-3100, a novel antagonist of the CXCR-4 chemokine receptor, in human volunteers., Antimicrob Agents Chemother 44 (2000) 1667-1673.

[53] C. Hendrix, A. Collier, M. Lederman, D. Schols, R. Pollard, S. Brown, J. Jackson, R. Coombs, M. Glesby, C. Flexner, G. Bridger, K. Badel, R. MacFarland, G. Henson, G. Calandra, A.H.S. Group, Safety, pharmacokinetics, and antiviral activity of AMD3100, a selective CXCR4 receptor inhibitor, in HIV-1 infection., J Acquir Immune Defic Syndr 37 (2004) 1253-1262.

[54] T. Nanki, K. Hayashida, H. El-Gabalawy, S. Suson, K. Shi, H. Girschick, S. Yavuz, P. Lipsky, Stromal cell-derived factor-1-CXC chemokine receptor 4 interactions play a central role in CD4+ T cell accumulation in rheumatoid arthritis synovium., J Immunol 165 (2000) 6590-6598.

[55] A. Müller, B. Homey, H. Soto, N. Ge, D. Catron, M. Buchanan, T. McClanahan, E. Murphy, W. Yuan, S. Wagner, J. Barrera, A. Mohar, E. Verástegui, A. Zlotnik, Involvement of chemokine receptors in breast cancer metastasis., Nature 410 (2001) 50-56.

[56] S. Abi-Younes, A. Sauty, F. Mach, G. Sukhova, P. Libby, A. Luster, The stromal cell-derived factor-1 chemokine is a potent platelet agonist highly expressed in atherosclerotic plaques., Circ Res 86 (2000) 131-138.

[57] A. Bazarbachi, R. Nasr, M. El-Sabban, A. Mahé, R. Mahieux, A. Gessain, N. Darwiche, G. Dbaibo, J. Kersual, Y. Zermati, L. Dianoux, M. Chelbi-Alix, H. de Thé, O. Hermine, Evidence against a direct cytotoxic effect of alpha interferon and zidovudine in HTLV-I associated adult T cell leukemia/lymphoma., Leukemia 14 (2000) 716-721.